Studies of young stars with accretion – and outflow-tracing spectral lines

L.V. Tambovtseva and V.P. Grinin

Main (Pulkovo) Astronomical observatory, St. Petersburg, Russia
www.gao.spb.ru

- Environment of young stars (TTSs and HAEBEs). Emitting regions
- How to choose geometric and physical model parameters of the emitting region
- Non-LTE modeling hydrogen emission lines
- Interferometry as a tool to constrain model parameters
- S Coronae Australis – a T Tauri Twin

In colloboration with:

G. Weigelt, K.-H. Hofmann, D. Schertl (MPIfR, Bonn, Germany)
S. Kraus, A. Kreplin (Exeter University, Exeter, UK)
A. Caratti o Garatti and R. Garcia-Lopez (DIAS, Dublin, Ireland)

Line emitting regions

Accretion

boundary layer (BLA)

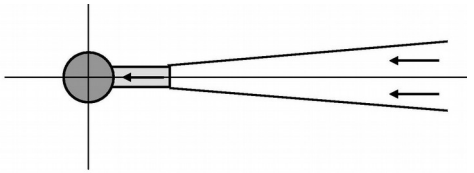

Magnetosheric (MA)

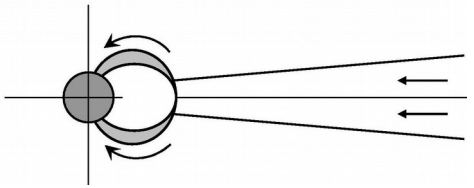

Outflow

stellar (polar) wind

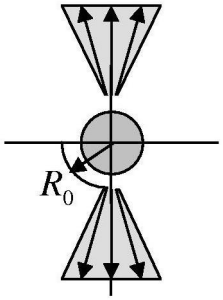

disk wind

Magneto-centrifugal

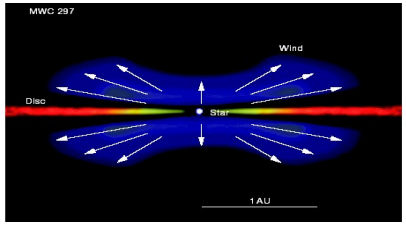

X-wind

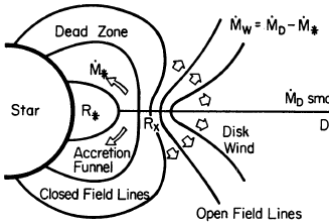

Conical

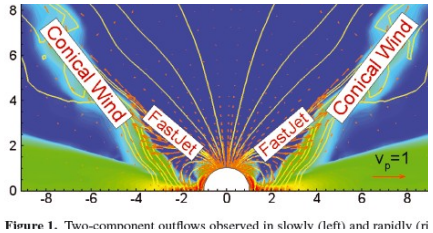

Photoevaporative

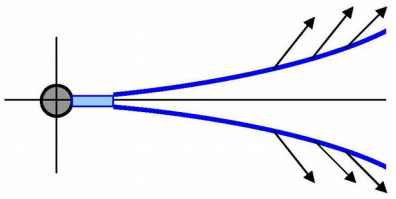

Line emitting regions

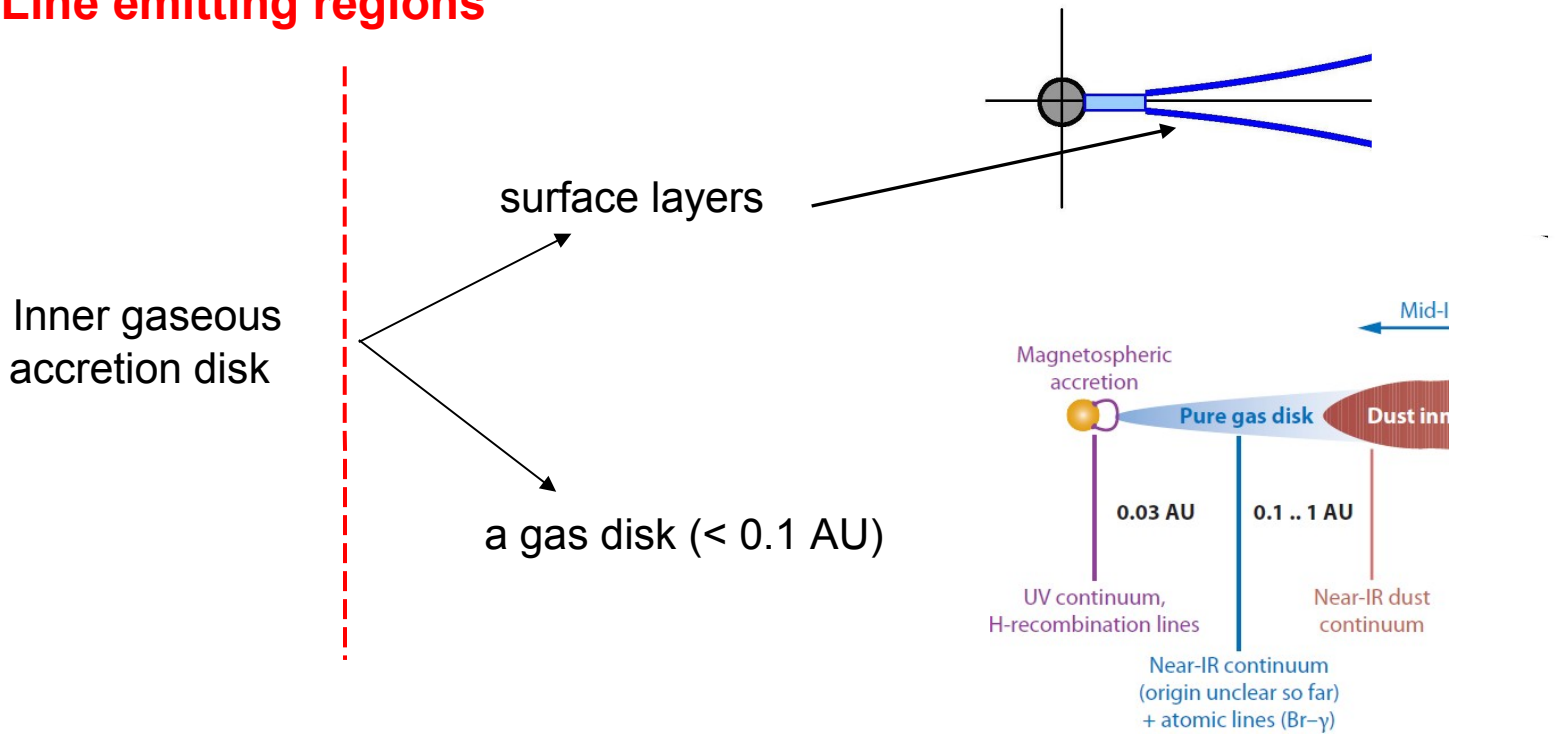

In order to distinguish between the contribution to the line profiles from different kinematic flows and derive quantitative measures it is required modeling the emission lines.

Inverse problem:

We know traces - some emission lines;
- inclination (sometimes);
- interferometric observables (not always)
- an additional information:
  (photometric or line variability, magnetic field, dust, etc.)

We have to determine:

- a geometrical structure of the region considered;
- physical mechanisms of inflow / outflow;
- an inclination angle

A choice of model parameters for the line emitting region

1. Kinematics → Line profiles observed

2. Geometry → Theoretical background

3. Size of emitting regions → Theoretical background
Interferometry

4. Constraint → Interferometry

5. Reliability of the model → Reproduction of several emission line profiles;
Reproduction of the line profile and all interferometric observables

Spectroscopic observations and analysis **have been and will be** an essential tool in discovering the intricate details in the formation of a classical T Tauri star and Herbig AeBe stars, as the spectral lines carry information on the kinematics and physical conditions of the gas close to the star *(Kwan & Fisher, 2011)*

Step 1

We divide it by several streamlines (SL) and solve mass continuity equations for each of them. As a result, we obtain a density and velocity distribution along of each SL.

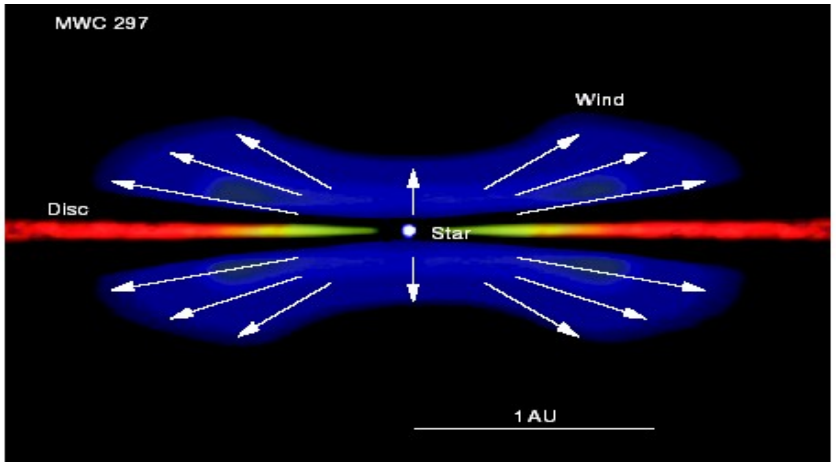

Tangential and poloidal velocity components are

In the corotation zone: $u(\omega)/u_K(\omega_i) \le f_c$

$$u(\omega) = u_K(\omega_i)(\omega/\omega_i)$$

In the zone of conservation of the angular momentum:

$$u(\omega) = u_K(\omega_i) f_c/(\omega/\omega_i)$$

$u_K(\omega_i)$ is the Keplerian velocity at a footpoint ω_i ,

f_c is a parameter

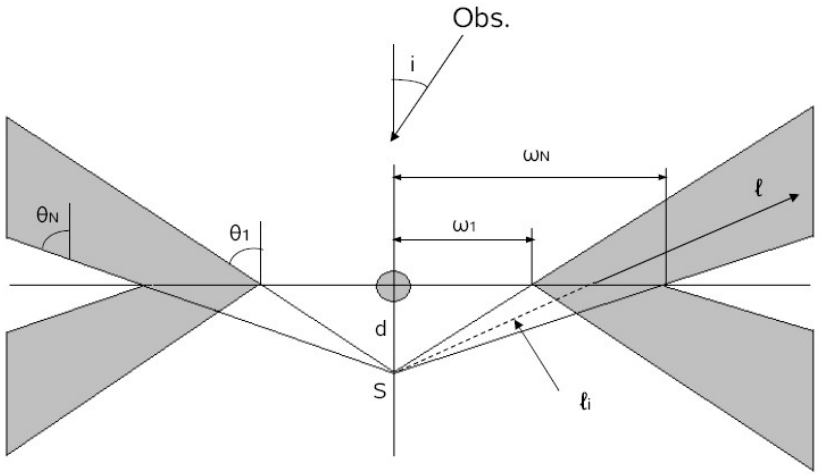

$$v(l) = v_0 + (v_\infty - v_0)(1 - l_i/l)^\beta$$

v_0, v_∞ are initial and terminal velocities for the i-th SL

$$\dot{m}(\omega) \propto \omega^{-\gamma}$$ a local MLR

$$\dot{M}_{wind} = 2\int_{\omega_1}^{\omega_N} \dot{m}(\omega) 2\pi\omega d\omega$$ a total MLR

Shlosman & Vitello (1993) (cataclysmic variables)
Kurosawa et al. (2006) (TTSs)
Murray & Chiang (1997) (galactic nuclei)
Grinin & Tambovtseva (2011) (HAEBEs)

Step 2: **We solve a system of the stationary equations**

$$\frac{dn_i}{dt} = R_i + Q_i = 0$$

n_i is the population of the *i*-th level,
R_i and Q_i are terms describing excitation and deactivation of an *i*-th level by radiation and collision.

$$i = 1,2,3 \ldots N_{atom}$$
(15 + continuum)

$$R_i = -n_i \left(\sum_{j=i}^{i-1} \left(A_{ij} + B_{ij} J_{ij} \right) + \sum_{k=i+1}^{\infty} B_{ik} J_{ik} + B_{ic} W J_{ic} \right) +$$
$$+ \sum_{k=i+1}^{\infty} n_k \left(A_{ki} + B_{ki} J_{ik} \right) + \sum_{j=1}^{i-1} n_j B_{ji} J_{ij}$$

$$Q_i = -n_i \left(n_e \left(q_{ic} + \sum_{i \neq j} q_{ij} \right) + B_{ci} W J_{ic} \right) +$$
$$+ n_e \sum_{j \neq i}^{\infty} n_j q_{ji} + n_e n^+ C_i + n_e^2 n^+ Q_{ci}$$

Radiative transfer codes:

Grinin & Katysheva 1980
Grinin & Mitskevich 1990
Tambovtseva et al. 2001

Radiative transition probabilities (Gershberg & Shnol 1974),
Collision transition probabilities (Johnson 1972, Scholz et al. 1990)

Intensity of the radiation:

$$J_{ik} = (1 - < \beta_{ik} >) S_{ik} + J^{\star}_{ik} W \beta^{\star}_{ik}$$

Source function:

$$S(r) = \frac{2h\nu^3}{c^2} \left(\frac{n_k(r)}{n_i(r)} \frac{g_i}{g_k} - 1 \right)^{-1}$$

Mean escape probability of the quantum in the line *ik* from the given point of the medium:

$$< \beta_{ik}(l,\theta) > = \int \beta_{ik}(r,l,\mathsf{s}) \frac{d\Omega}{4\pi} ,$$

$$\beta_{ik}(l,\theta,\mathsf{s}) = \frac{1 - e^{-\tau_{ik}}}{\tau_{ik}}$$

The integral is taken over all solid angles Ω (ℓ,θ)

The effective optical depth of the emitting region at the point with co-ordinates (ℓ,θ):

$$\tau_{ik}(l,\theta,\mathsf{s}) = \kappa_{ik}(l,\theta)\, v_t \left| dv_{\mathsf{s}}/ds \right|^{-1}$$

SEI = Sobolev + Exact Integration

$$I_w(\nu) = \int_A I_w(\nu,x,y)\, dx\, dy$$

$$I_w(\nu,x,y) = \int_{z_{min}}^{z_{max}} S(\mathsf{r})\, \phi(\nu - \nu_0 \frac{\mathsf{v}_z(\mathsf{r})}{c})\, e^{-\tau(\nu,\mathsf{r})}\, \kappa(\mathsf{r})\, dz$$

Grinin & Tambovtseva 2011

1. A temperature law

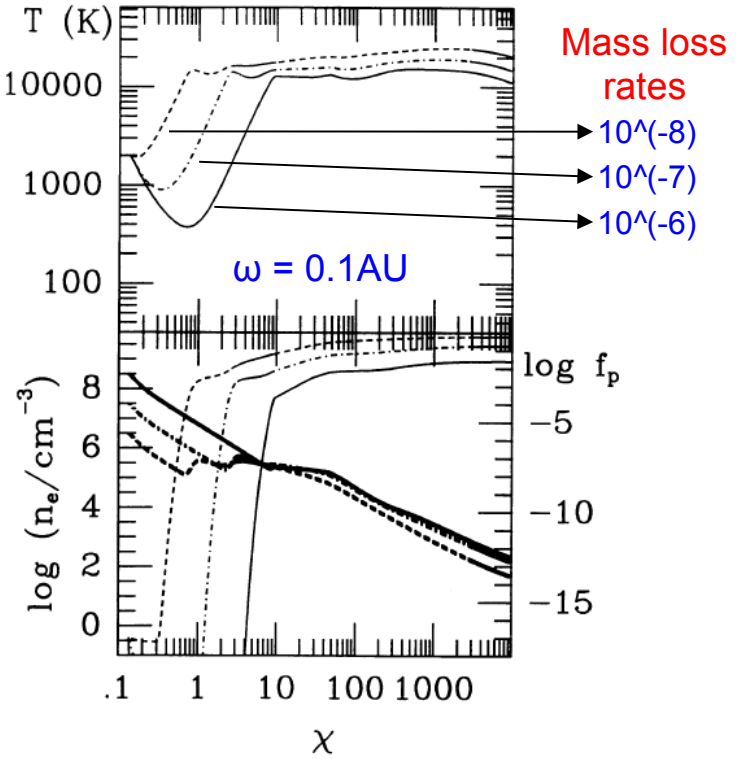

A gas temperature along a flow line

2. A corotation zone

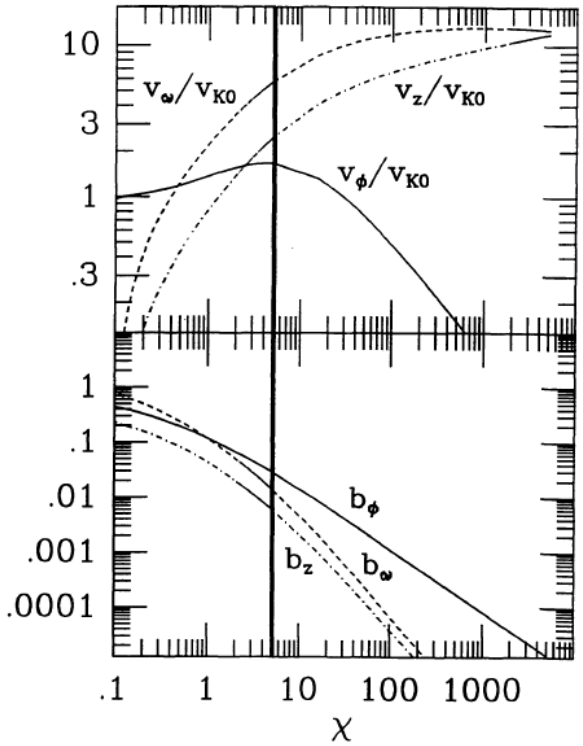

A velocity along a flow line in units of the Keplerian velocity at the footpoint

Safier 1993
Garcia et al. 2001

3 . An influence of the radiation (for HAEBEs)

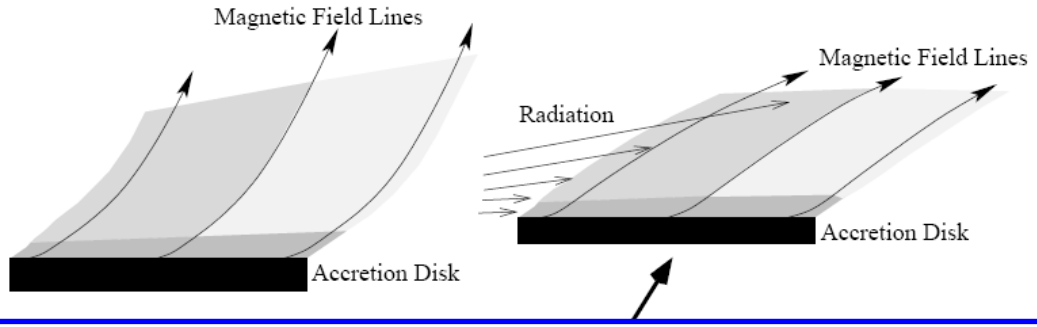

De Kool & Begelman 1995;
Drew et al. 1998;
Everett et al. 2001

When modeling we have to take into account that

- a part of the star radiation is absorbed by the MA-region;

- a part of the MA radiation is absorbed by the disk wind;

- a disk continuum can be partially absorbed by the disk wind

- a base of the disk wind has to be excluded from the consideration because of the low gas temperature

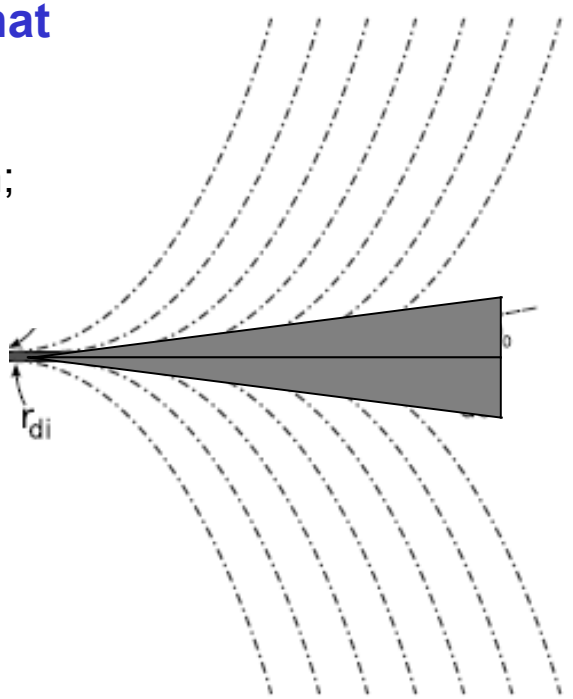

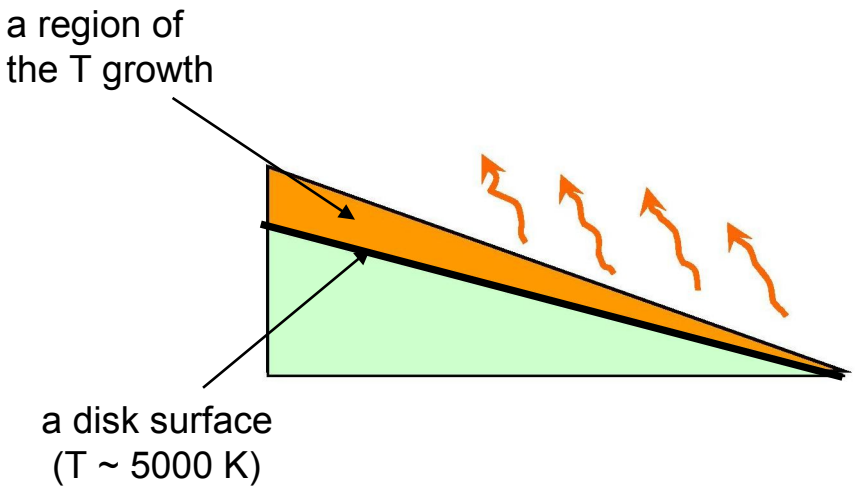

Weigelt et al. 2011, A&A

MWC 297
Herbig Be star
SpT B1.5V

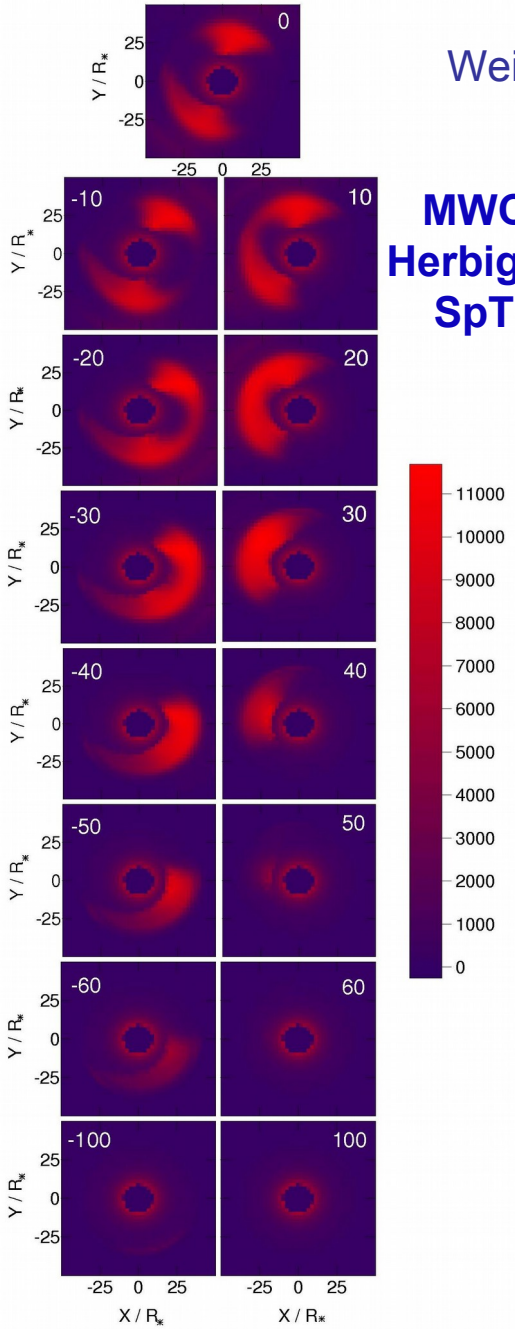

Disk wind images at different radial velocities (in km/s)

Disk wind model

M_w $10^{-8}\ M_\odot/yr$	θ_w deg.	ω_1 r_*	ω_N r_*	γ
10	80	17.5	35	2

spectrum

visibilities

wavelength-differential phases

closure phase

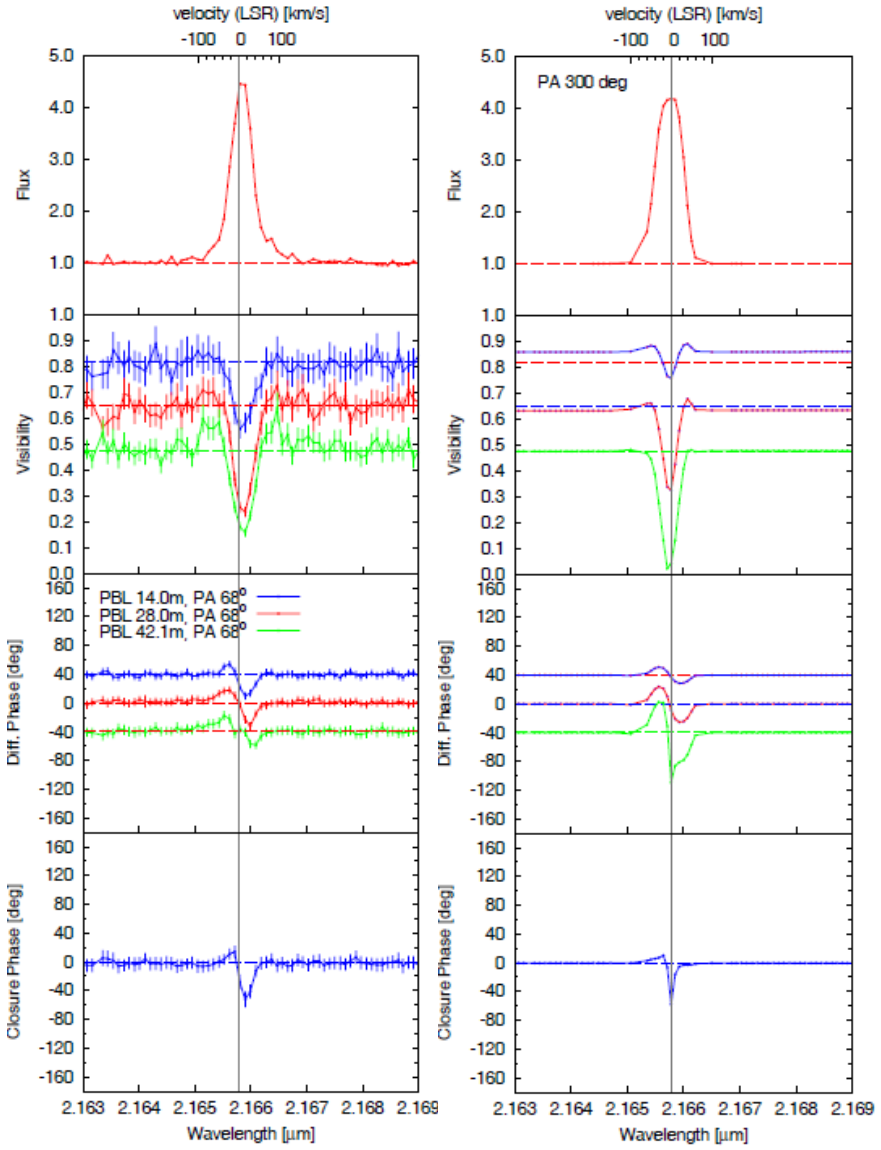

Observed and model quantities

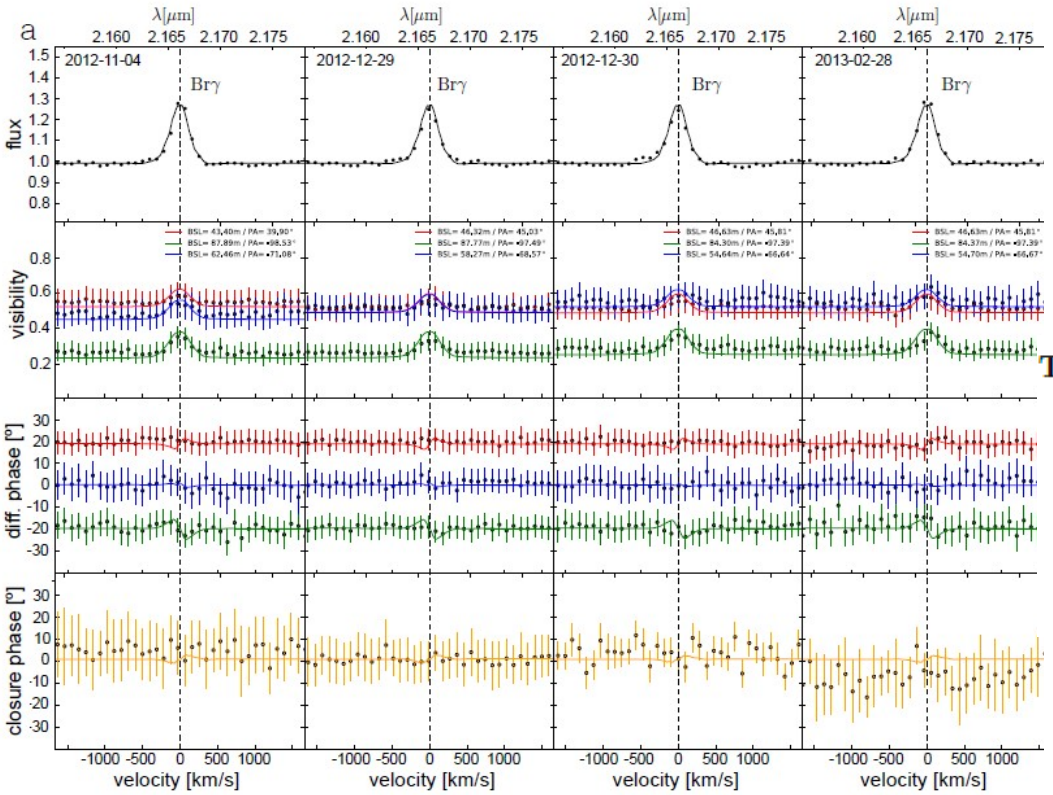

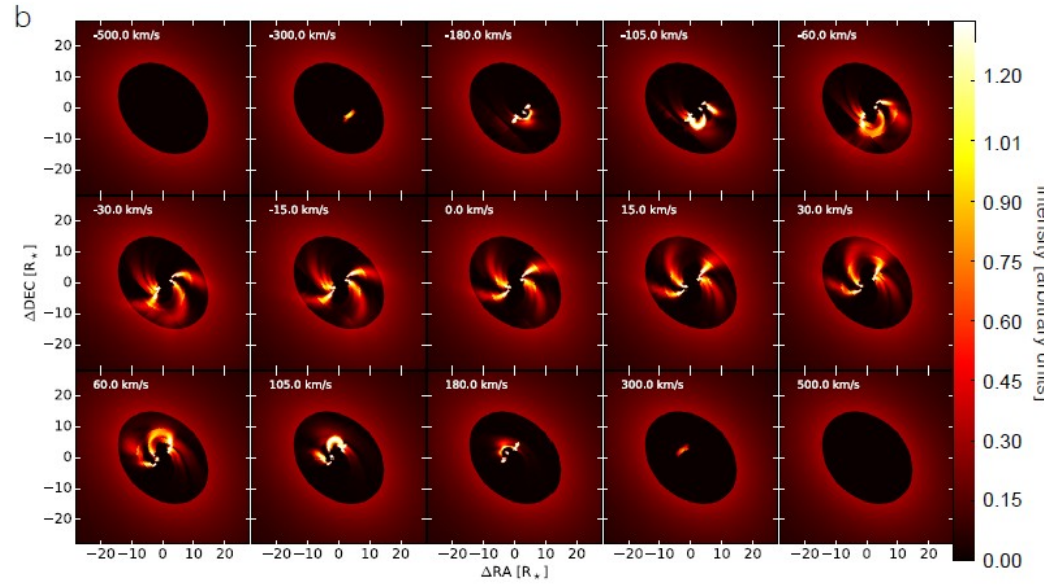

MWC 120 (HD 37806)

Table 4. Best model parameters of the disc wind

θ_1 [°]	θ_N [°]	ω_1 [$R_\star$]	ω_N [$R_\star$]	γ	β	$\dot{M}$ [$M_\odot$ yr^{-1}]	i [°]	PA [°]
45	79	2	10	3	5	10^{-7}	40	135

R_{in} — the inner boundary of the disk wind launching region

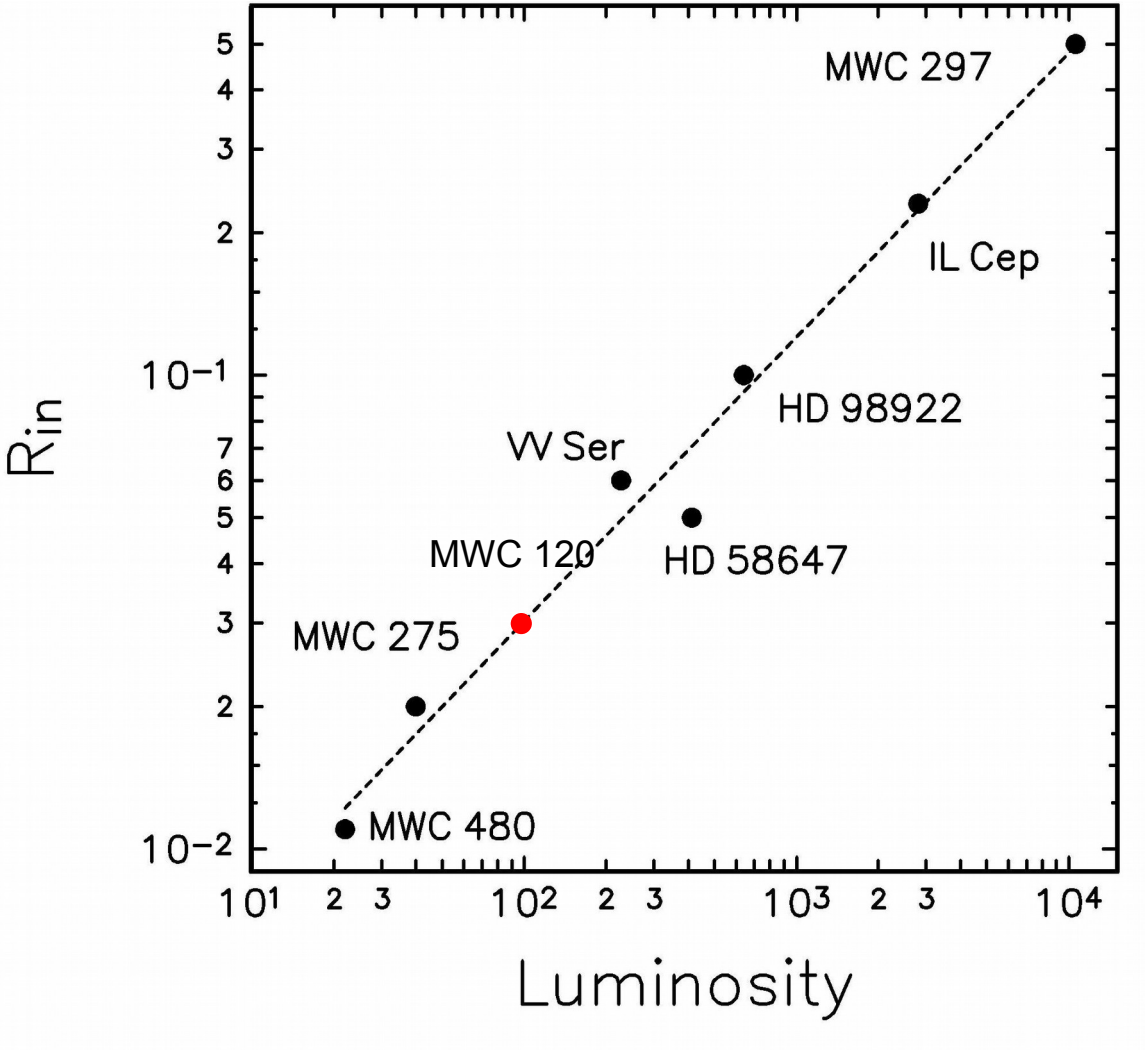

Probably increasing effect of the radiation pressure onto the disk wind

Vink et al. 2002,
Ababakr, Oudmaijer & Vink 2017:

(a change in a linear polarization
In the Hα lines in HAEBEs)

MA – magnetospheric accretion

BLA – Boundary layer accretion

Sp = B7 – B8

MA | MA | BLA ?

Low-mass stars, slow rotators

Luminous intermediate-mass stars, rapid rotators

T Tauri stars

Herbig Ae stars

Herbig Be stars

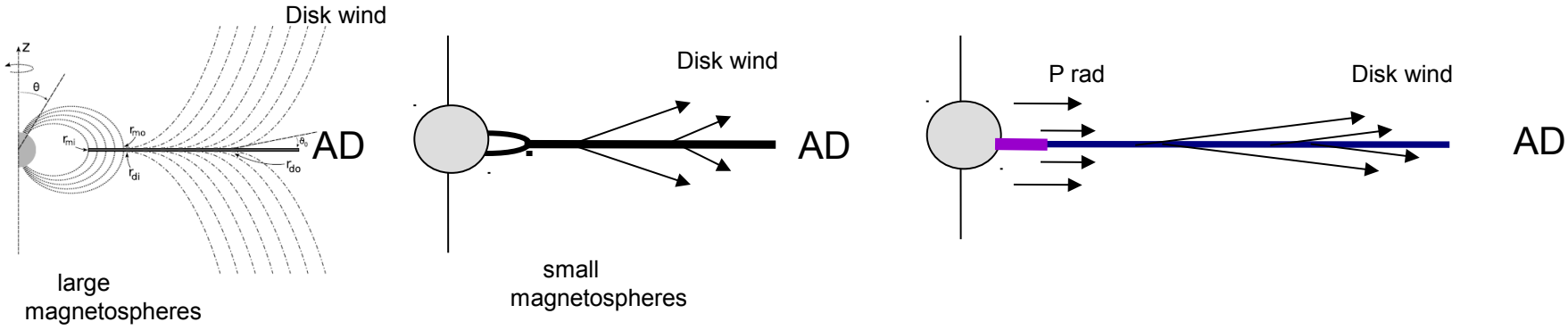

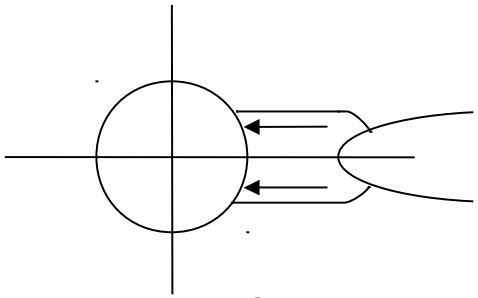

B. Flat-like magnetosphere (boundary layer accretion) rotating gas, free-fall motion (HAEBEs)

$$v(r)\frac{dv}{dr} = -\frac{GM}{r^2} + \frac{u^2(r)}{r} \qquad \dot{M} = 2\pi r h v \rho(\mathrm{r})\mathrm{v}(\mathrm{r})$$

UXORs

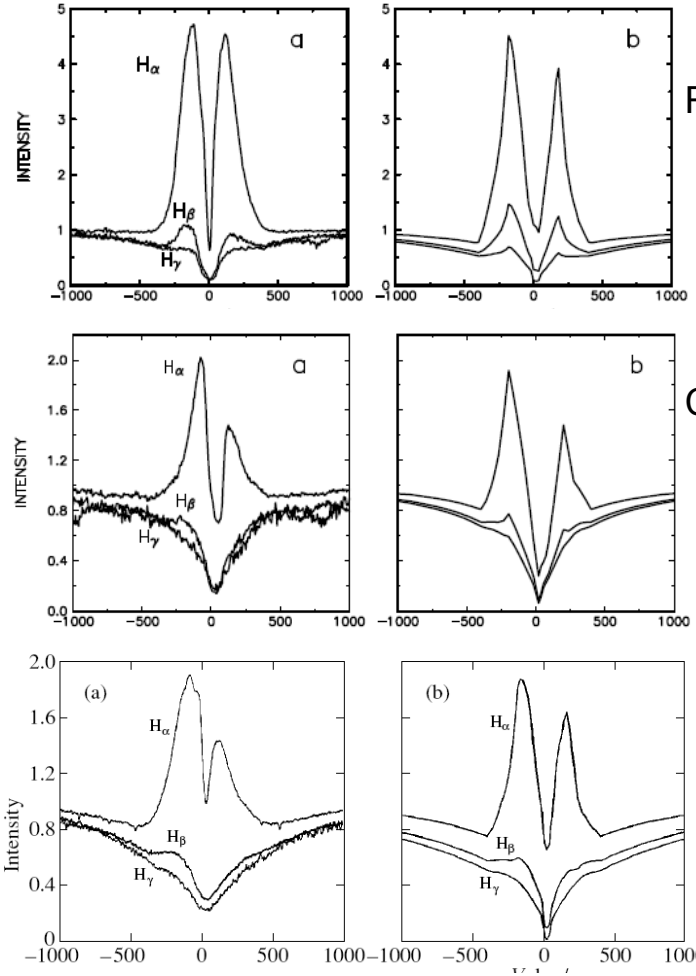

Disk accretion + gaseous disk

$$\frac{\dot{M}_w}{\dot{M}_{acc}} = 0.1$$

MWC 480 : disk accretion + disk wind

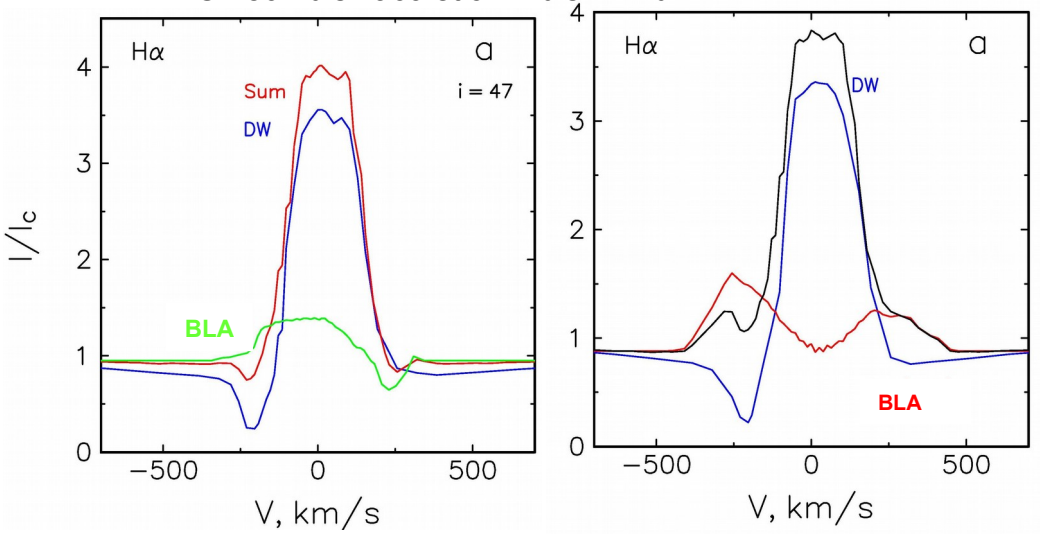

Model description and results: Tambovtseva + 2014, 2016 (A&A),

UXORs and MWC 480: 1999, 2001, 2016 (Astron. Let.)

A. magnetospheric accretion

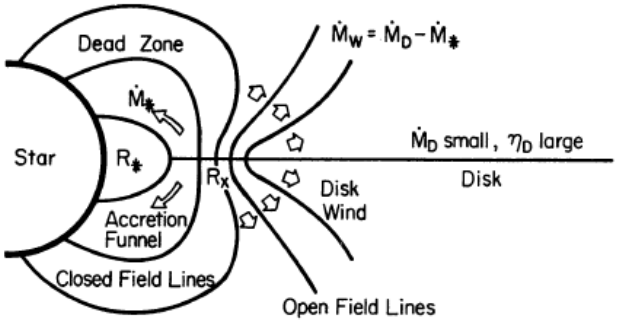

Shu et al. 1994

$$\frac{\dot{M}_w}{\dot{M}_{acc}} = 0.1$$

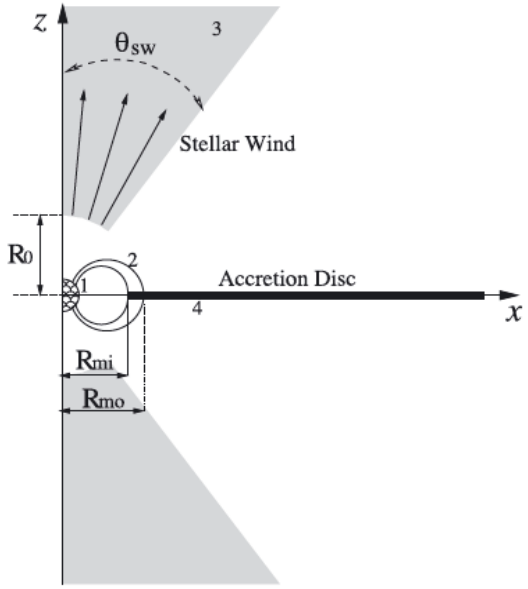

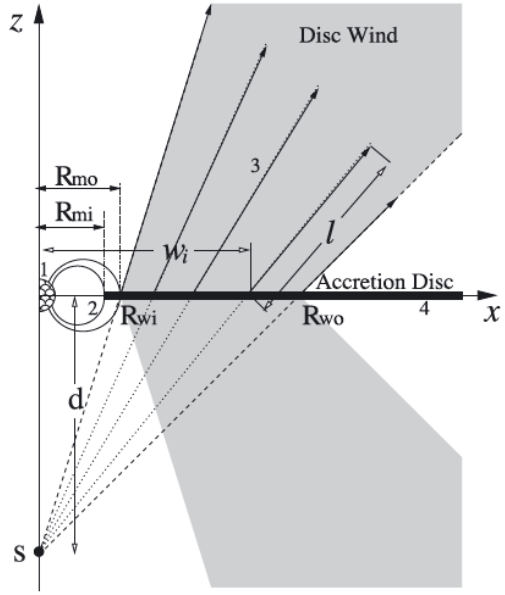

e.g., Calvet et al. 1992, Hartmann et al. 1994, Muzerolle et al. 1998, 2001, 2004,
Kurosawa et al. 2006, 2011, 2016,
Mendigutia et al. 2011, Lima et al. 2010,
Gahm et al. 2018

A&A 2018

S Coronae Australis - a T Tauri Twin ⋆

G. F. Gahm[1], P. P. Petrov[2], L. V. Tambovtseva[3], V. P. Grinin[4], H. C. Stempels[5], and F. M. Walter[6]

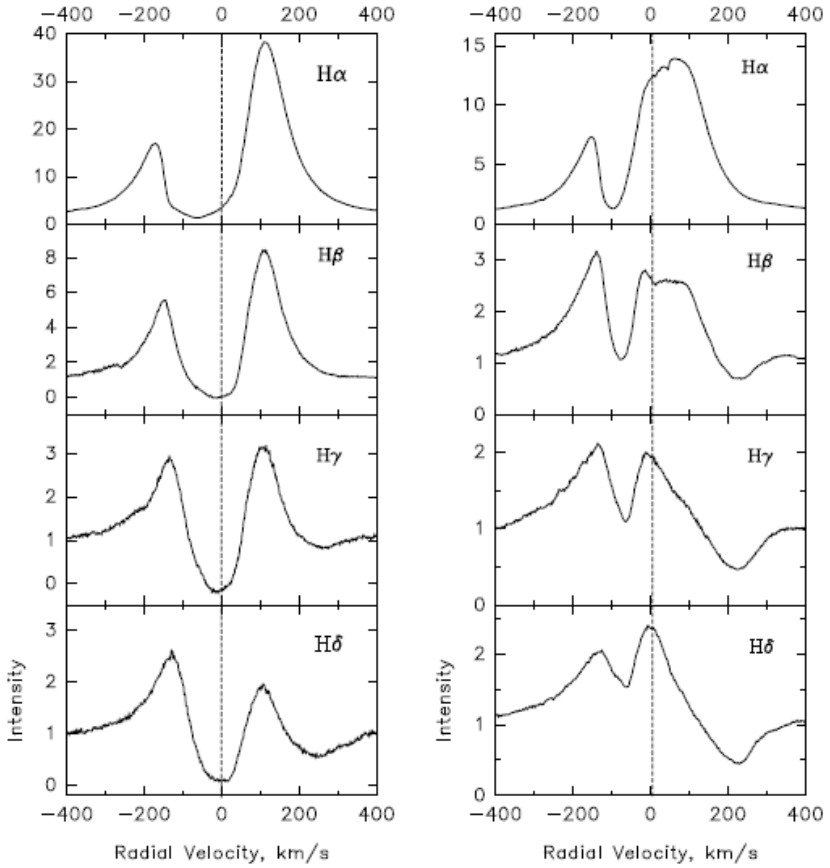

Fig. 4. Balmer line profiles. Left: S CrA NW, right: S CrA SE. All line intensities are normalized to the continuum level.

Table 1. Stellar parameters

	SE component	NW component
v_{rad} (km s^{-1})	-0.5 ± 3.9	+0.9 ± 2.5
v sin i (km s^{-1})	12	12
T_{eff} (K)	4250	4250
log g	4.0	4.0
mean veiling factor	3.3	8.3

S Cra N Brγ profile as observed in 1994 at IRTF

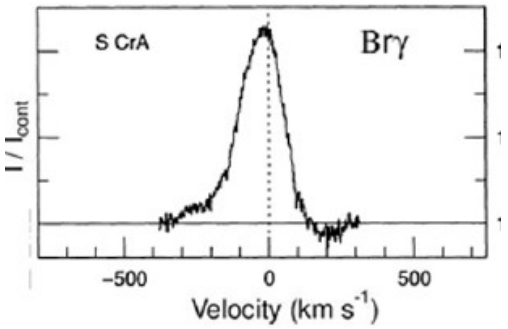

Najita et al. 1996,

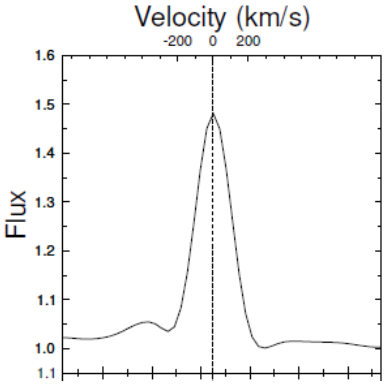

Garcia Lopez +, 2017

VLTI - GRAVITY

(i =28±3° and i =22±6°)

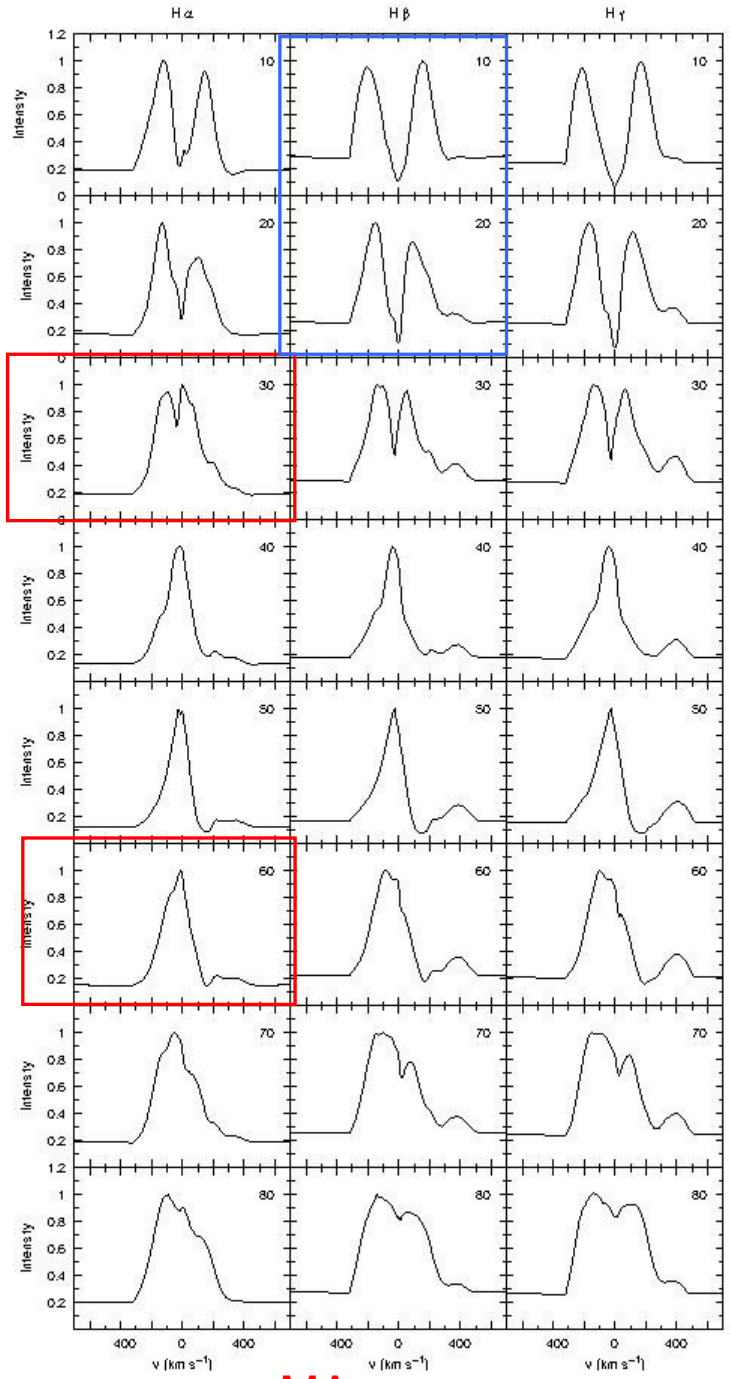

MA

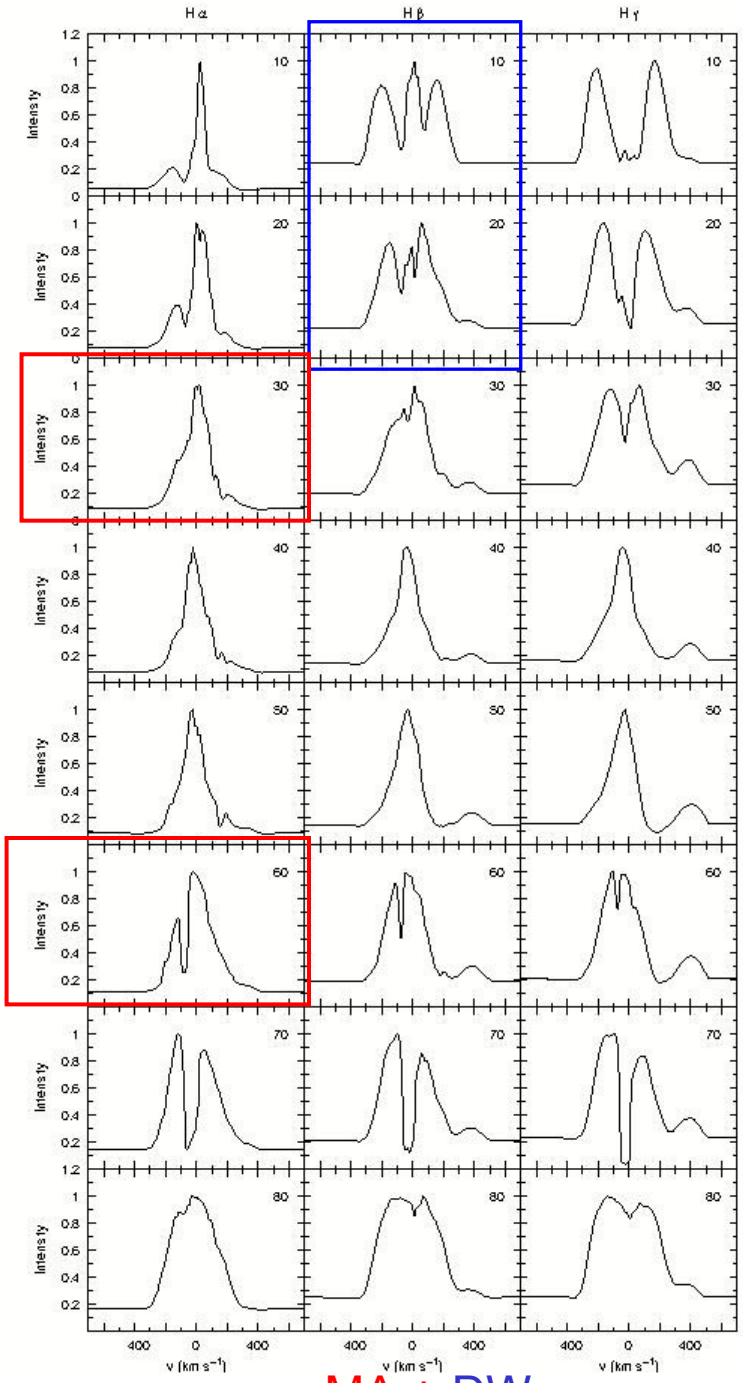

MA + DW

Line profiles are normalized to the peak intensities

Components of the line profile:

MA

DW

Total

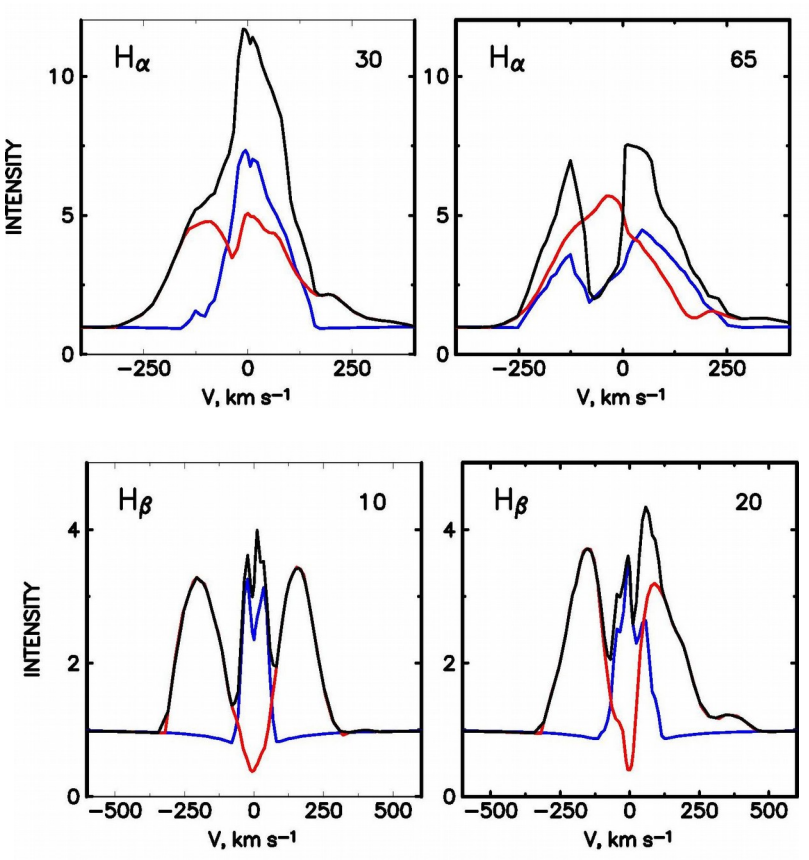

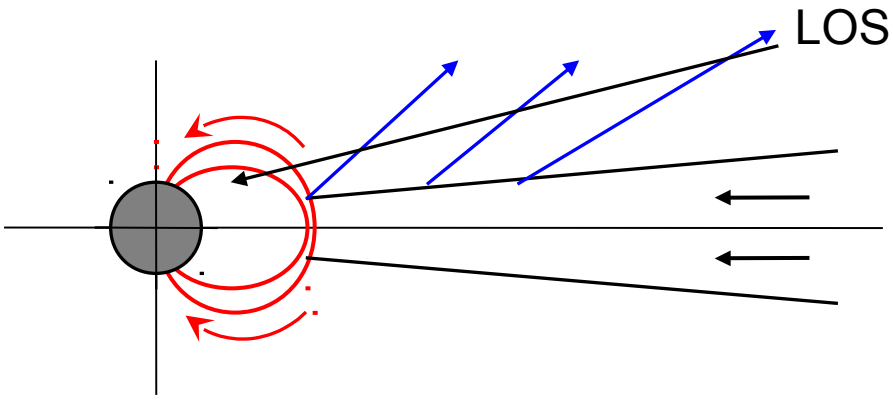

Table 4. Parameters of the magnetospheric accretion model

Model	R_{out} R_*	$\theta_{in} - \theta_{out}$ degrees	T_{R_*} K	α	$\dot{M}_{acc}$ $M_\odot$ yr^{-1}
MA1	5	40 - 60	10000	3	5×10^{-7}
MA2	5	20 - 45	8000	3	5×10^{-7}

Table 3. Parameters of the disk wind model

name	$w_1 - w_N$ R_*	θ_1 degree	f	γ	$\dot{M}_w$ $M_\odot$ yr^{-1}	β	T K
DW1	5 - 20	45	5	2	5×10^{-9}	5	8000
DW2	5 - 20	45	5	2	5×10^{-8}	5	8000

Line profiles are normalised to the continuum

S CrA SE DW1 + MA1 (i = 65°)

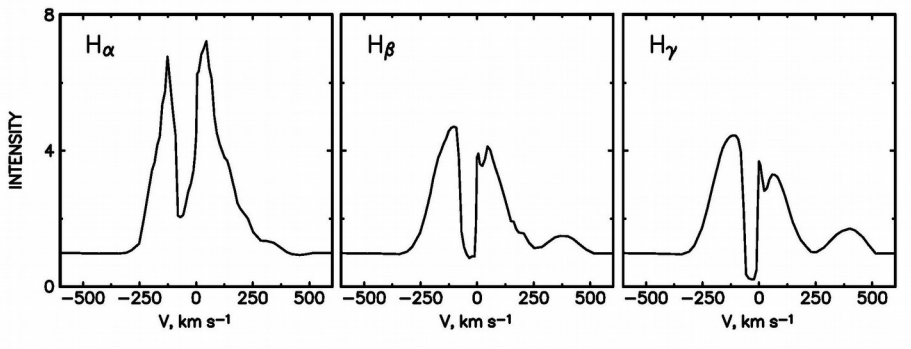

i = 65

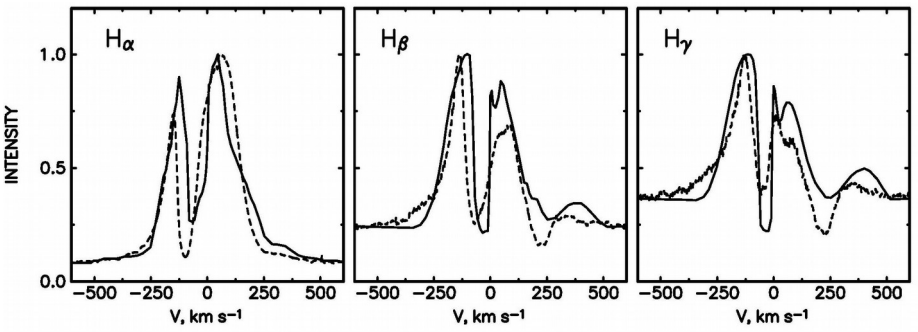

S CrA NW DW2+ MA2

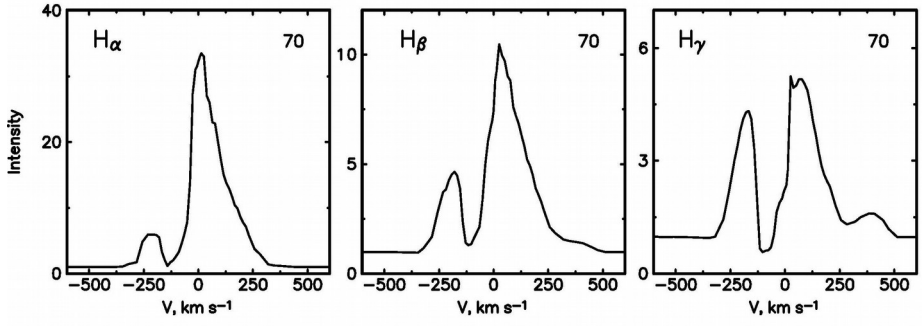

i = 60

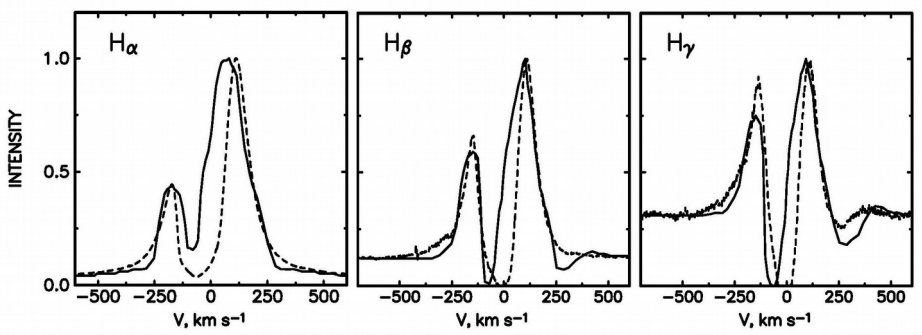

Conclusion

1. Unlike the TTS stars, in the Herbig AeBe stars a contribution of the radiation from a magnetospheric accretion or a polar wind into the hydrogen line emission is small; the disk wind is a dominant contributor.

1. Combination of the accretion/wind model parameters and inclinations permits us to obtain a large variety of profile shapes. Calculation of the interferometric functions together with the emission lines modeling gives constraints to the model parameters and provides us an additional information about a star+disk system (size, inclination, etc.).

1. A type of accretion onto the Herbig Be stars can differ from that onto the TTSs or Herbig Ae stars. An accretion is able to change significantly the shape of Balmer lines in HAEBEs leaving it, however, with “an outflow” features (i.e., one will not see traces of the accretion).

1. Inclination angles obtained with the data on different wavelengths can be different. It may be caused by a presence of the dust lifting with the disk wind.

1. The IR Brγ lines are formed in the regions close to the star and to the disk wind base. In the very base of the disk wind the gas T is not so large to lead to this transition. Excluding this narrow layer from consideration, we reduce a rotation velocity component, a poloidal velocity is still small. In most cases this leads to a single line profile. (Double-peaked Brγ line profiles may be formed at the rapid increase in the gas temperature).

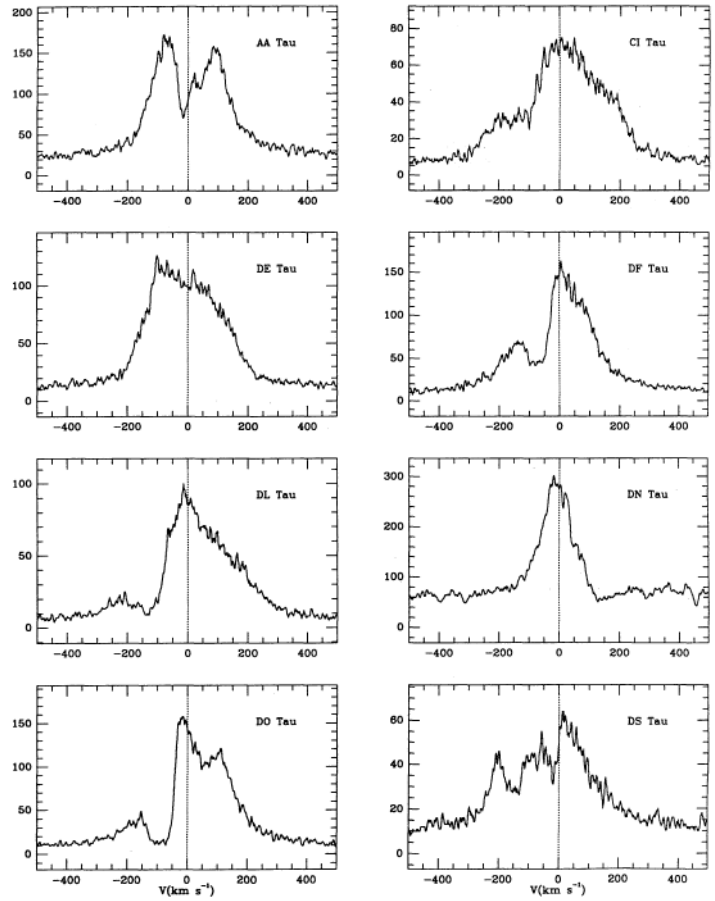

es of T Tauri stars, obtained with the FLWO 1.5 m echelle spectrograph and intensified Reticon detector on JD 2
over the resolution of approximately 12 km s^{-1}. Further details of the instrumentation are given by Latham (1982)

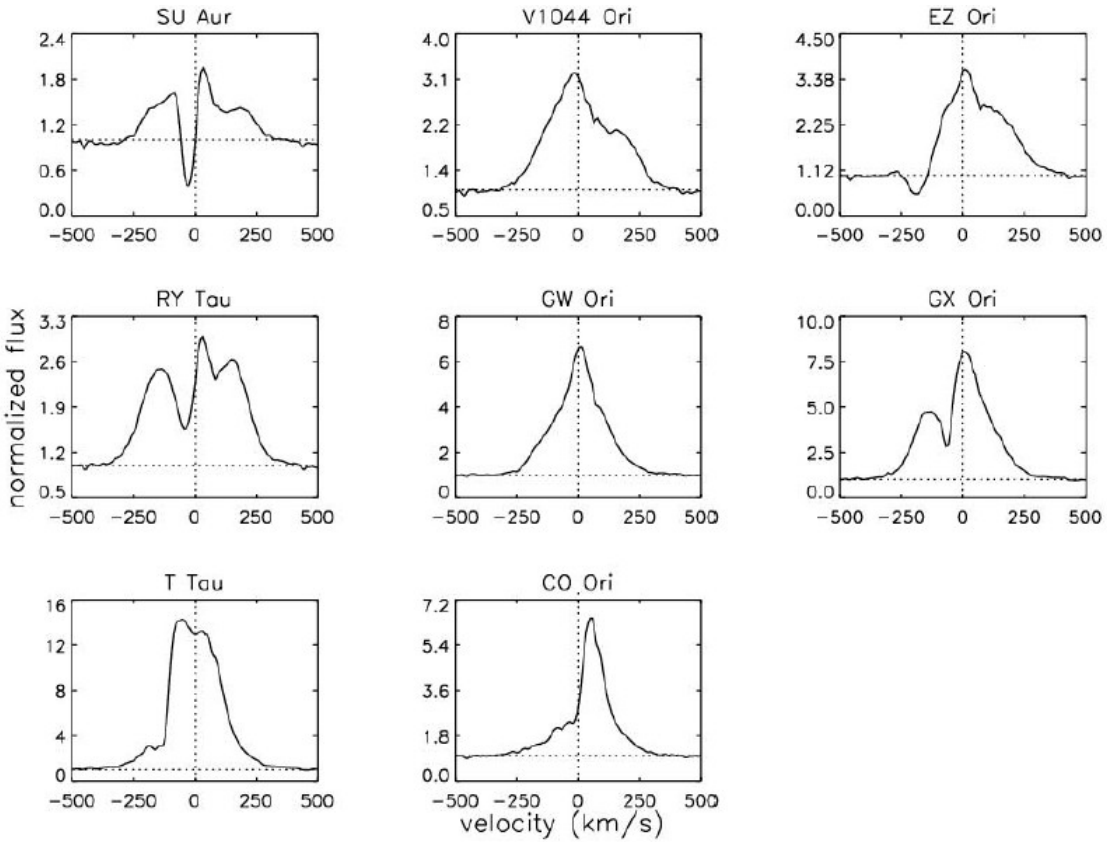

FIG. 12.—Hα line profiles of IMTTSs normalized to the continuum. Stars are identified in each plot.

Stellar wind as a by-product

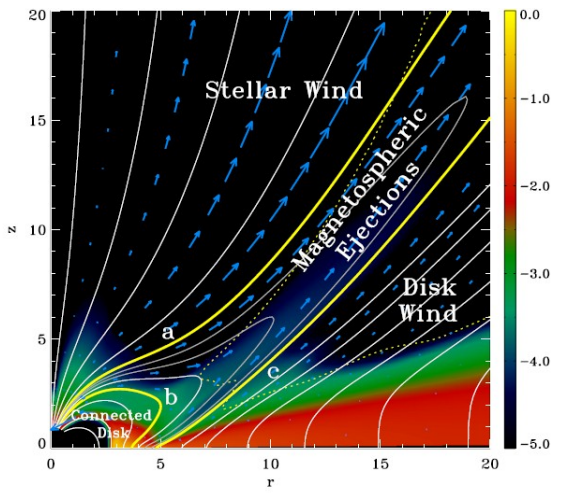

Fig. 1. Global view of the star-disk interacting system. A logarithmic density map is shown in the background. Poloidal speed vectors are represented as blue arrows. The dotted line marks the Alfvén surface, where $u_p = B_p/\sqrt{4\pi\rho}$. Sample field lines are plotted with white solid

Zanni & Ferreira 2013 ~ 5% $\dot{M}$_acc

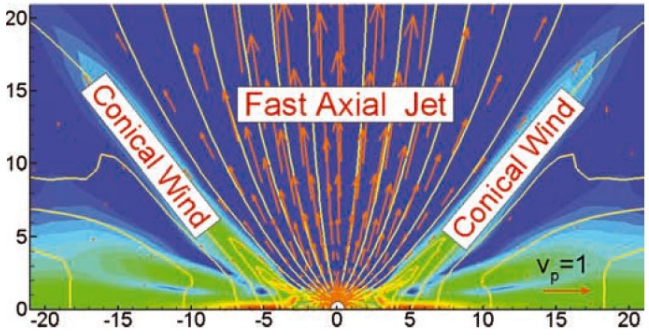

Romanova et al. 2009

Accretion driven stellar wind

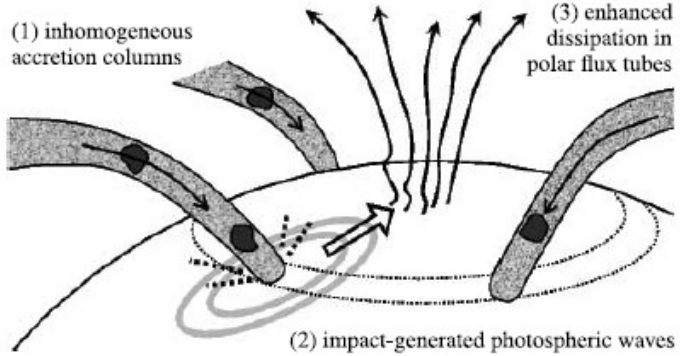

Matt & Pudritz 2007, Cranmer 2009 ~ 1% M_acc

Petrov et al. 2014

V 1331 Cyg, Hα,β line modeling

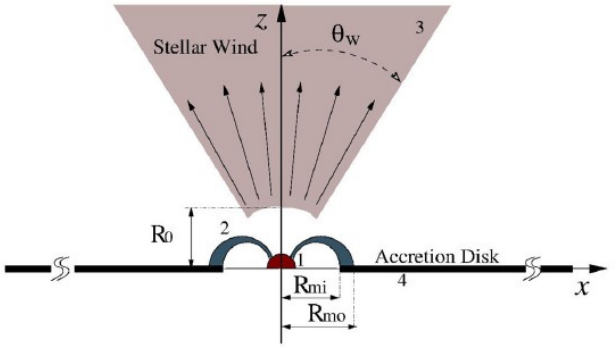

Table 3. Model parameters for line fits.

Model ID	$\dot{M}_w$	θ_w
...	($\dot{M}_\odot$ yr^{-1})	...
A	6.0×10^{-8}	50°
B	9.0×10^{-8}	50°
C	1.1×10^{-7}	50°

$\dot{M}_a$ ($\dot{M}_\odot$yr^{-1})	T_w (K)	v_∞ (km s^{-1})	v_0 (km s^{-1})	β ...	R_0 (R_*)
2×10^{-6}	9000	530	10	1.8	3.8

Hot polar wind in young stars = accretion driven wind

Matt & Pudritz (2007), Cranmer (2008)

Theoretical prediction

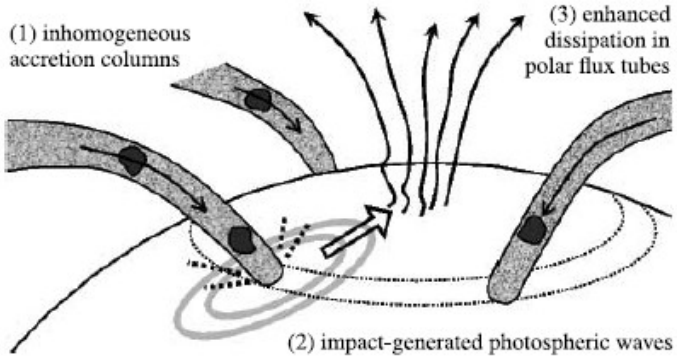

Sketch of the model

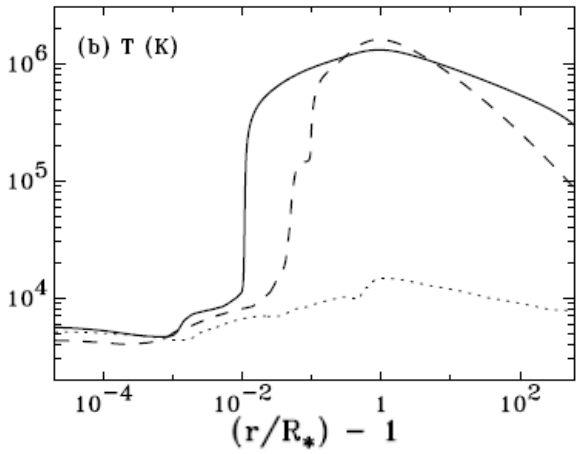

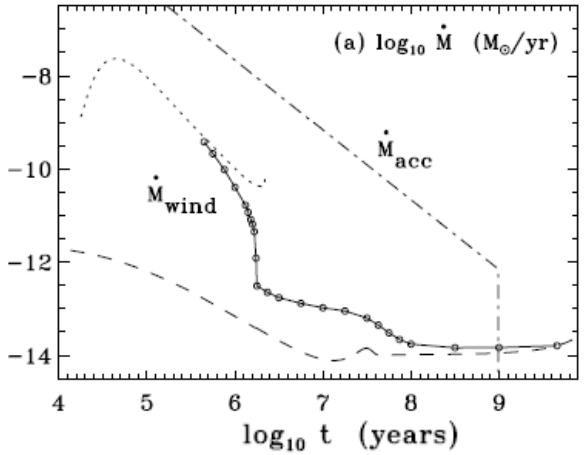

Physical mechanism:

An accretion driven wind from the polar regions of TTSs.

A convection – driven MHD turbulence (a solar coronal heating) + another source of the wave energy that is driven by the impact of plasma in neighboring flux tubes undergoing magnetospheric accretion

Result:

Rapid heating the wind (T ~ 10^6 K)

Models with T = (10 000 - 15 000) K and the mass loss rate $10^{-9} M_{SUN}$ /yr (~ 0.01 of an accretion rate) are suitable for emission lines formation

The pre-FUor V1331

As TW Hya, V1331 Cyg is observed pole-on

Petrov et al. 2014

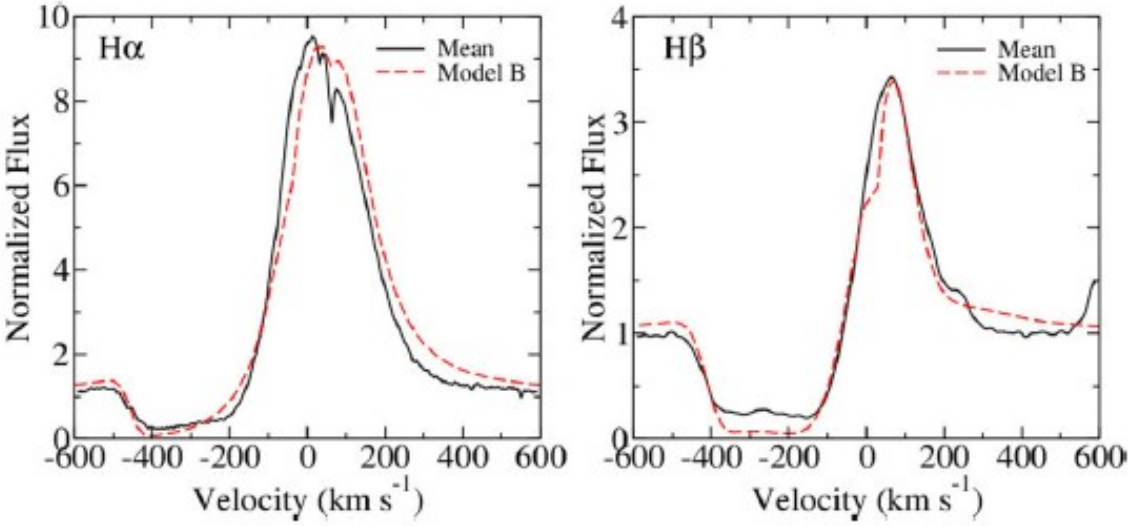

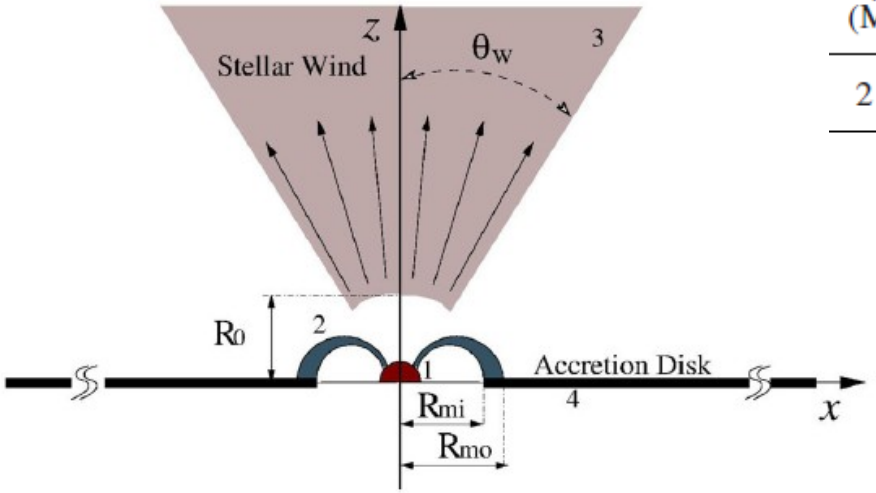

$\dot{M}_a$ ($M_\odot$ yr^{-1})	T_w (K)	v_∞ (km s^{-1})	v_0 (km s^{-1})	β ...	R_0 (R_*)
2×10^{-6}	9000	530	10	1.8	3.8

Table 3. Model parameters for line fits.

Model ID ...	$\dot{M}_w$ ($M_\odot$ yr^{-1})	θ_w ...
A	6.0×10^{-8}	50°
B	9.0×10^{-8}	50°
C	1.1×10^{-7}	50°

TTS TW Hya Dupree + 2014

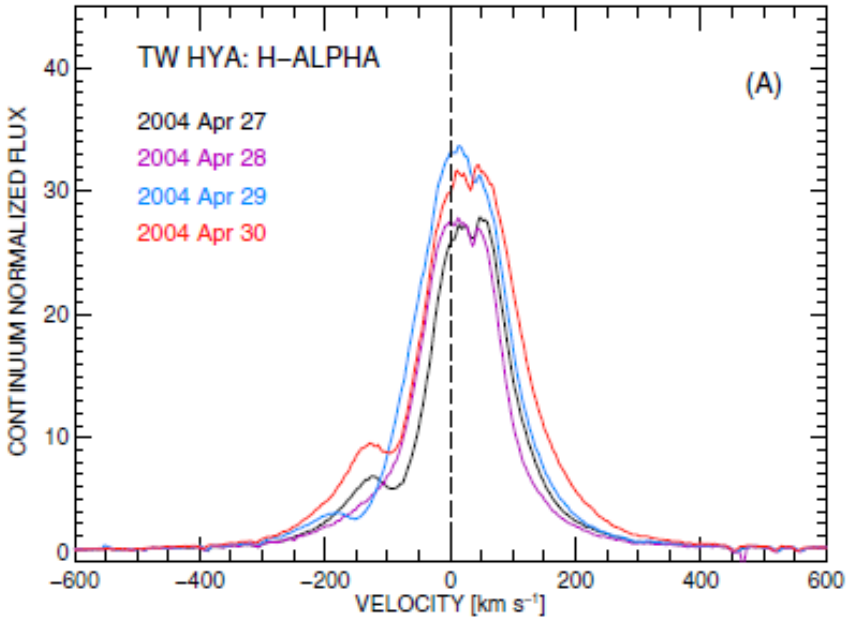

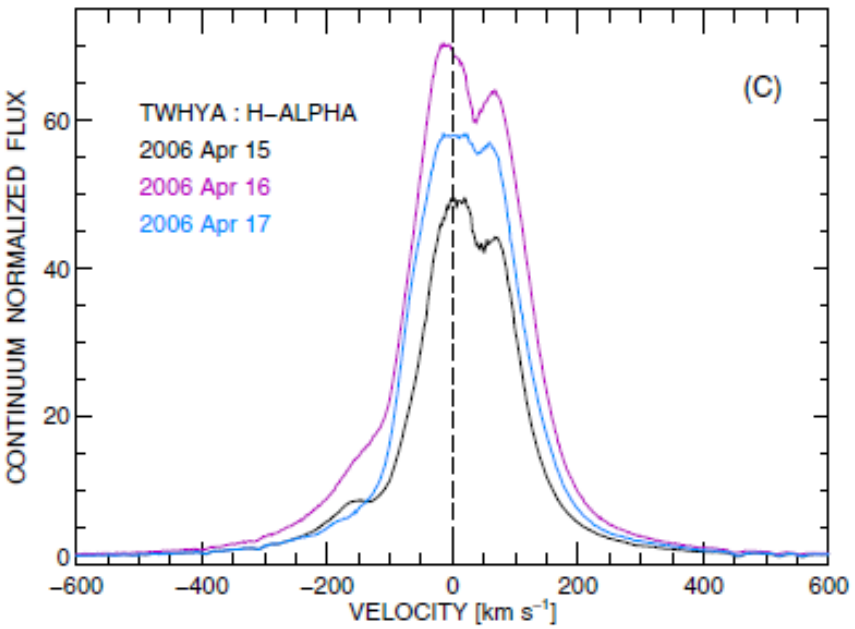

He I 10830

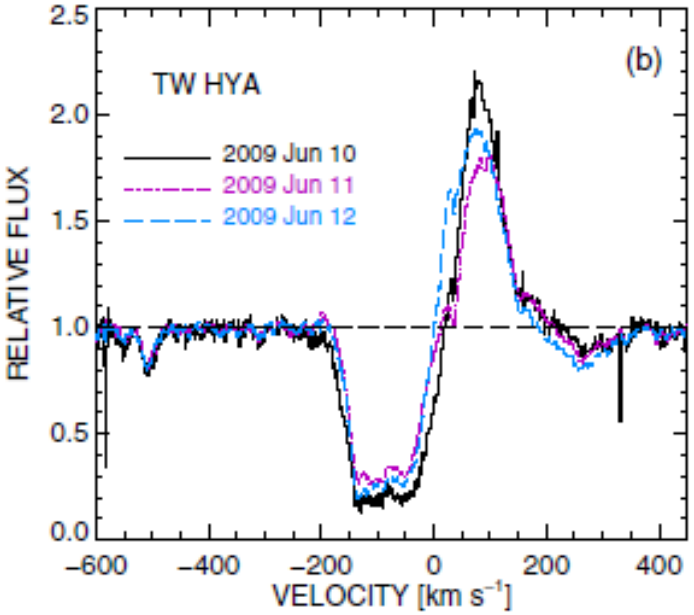

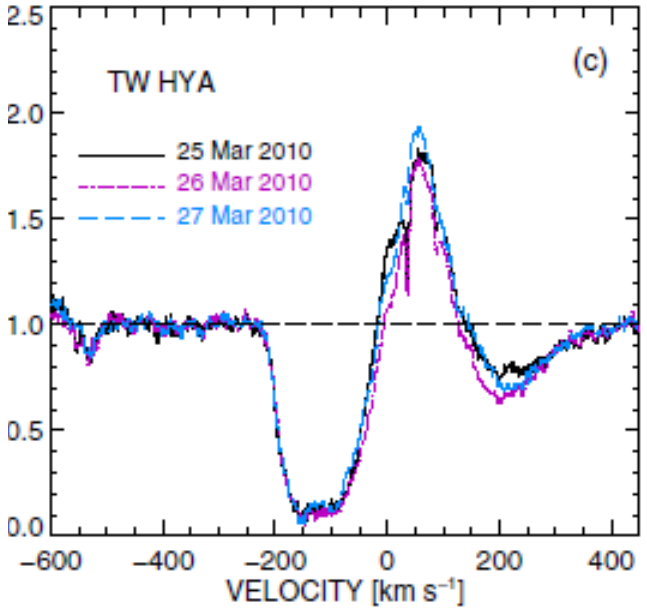

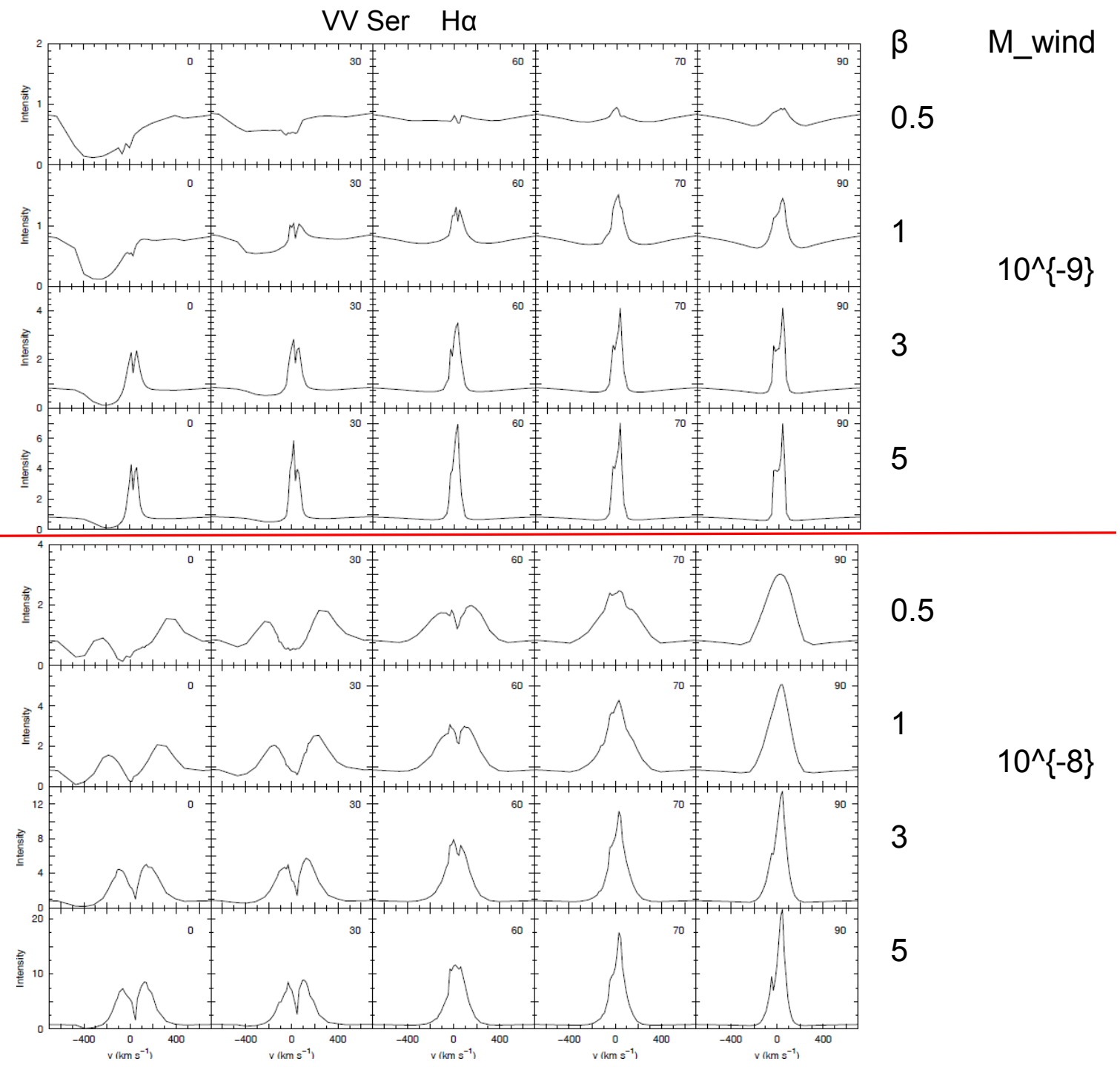
VV Ser Hα
β
M_wind
0.5
1
10^{-9}
3
5
0.5
1
10^{-8}
3
5
Intensity
v (km s^{-1})
0
30
60
70
90

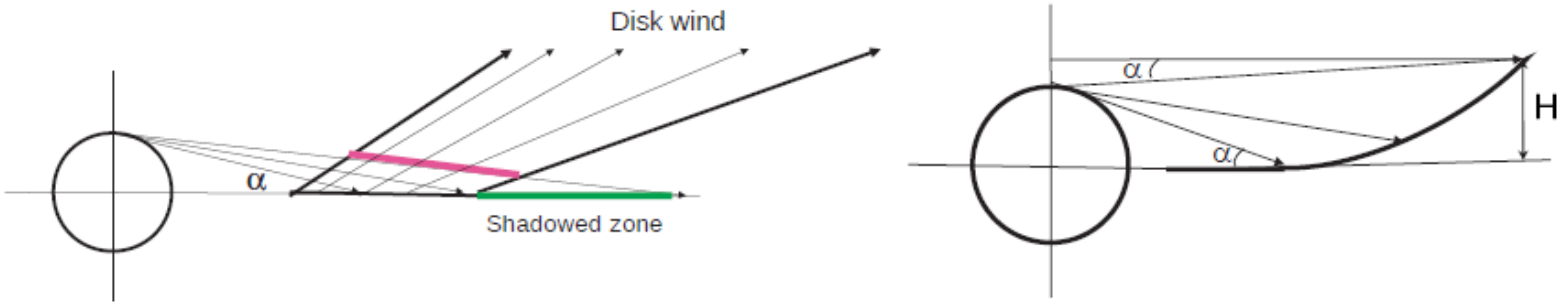

Fig. 4. Left: Sketch of the absorption of the hard stellar radiation (red line) by the disk wind. The green line is a shadow zone. Right: Points on the disk surface. Not to scale. See details in the text.

HD 98922

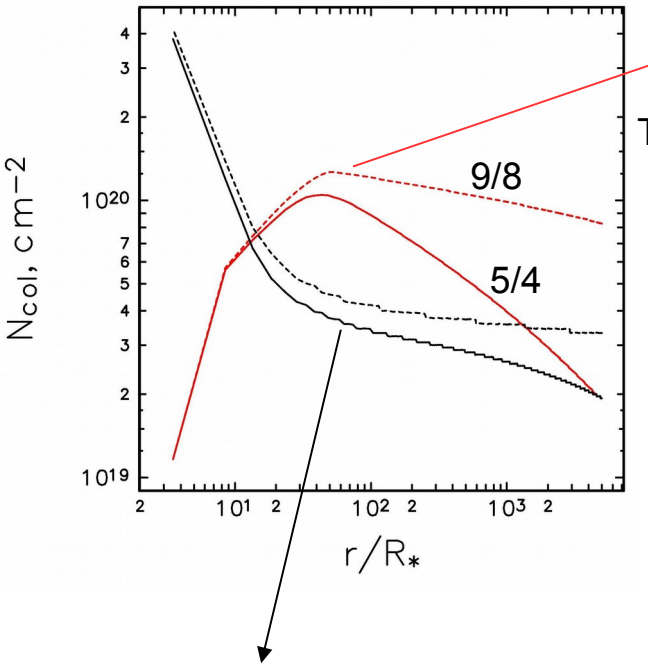

The disk wind is transparent for X-rays (0.3 – 1 kev) $N_X \approx 10^{21} - 10^{22}\,\mathrm{cm}^{-2}$

and FUV (6 – 13.6 ev) $N_{FUV} > 10^{22}\,\mathrm{cm}^{-2}$

The disk wind is opaque for EUV (> 13.ev) $N_{EUV} \approx 10^{17} - 10^{18}\,\mathrm{cm}^{-2}$

HD 163296 (MWC 275)

MWC 480 (Sp = A5e IV) and IL Cep (Sp = B2e IV-V) -
- photometrically low active Herbig AeBe stars.

van den Ancker +, 1998; Vink +, 2002; Kozlova +, 2003; Grady +, 2010; Alecian +, 2013; Mendigutia +, 2013 ; *Izmailov +, 2013*;

MWC 480 | T_ef = 8200 K; M = 1.9 M_sun; V sin i = 100 km/s; i = 30-50 deg - from *Grady* + 2010 | -from *Alecian* + 2013

IL Cep – binary star (sep. 6")

| M = 5 M_sun
T_ef = 19000 K
V sini = 180 km/s
i = ? | -from *Alecian* + 2013

The spectroscopic observations of the Herbig Ae star MWC 480 were performed by D. E. Mkrtichian on December 2014 with the 2.4-m telescope of the Thai National Observatory (TNO) equipped with the MRES echelle spectrograph. IL Cep — on December 2015.

MWC 275 (HD 163296)

Herbig Ae star

SpT A1V i = 38°

Garcia Lopez et al. 2016, A&A

Parameters[a]	Range[b]	MW6[b]
Temperature (K)	8000 – 10 000	10 000
Half opening angle (θ)	30° – 45°	45°
Inner radius ($\omega_1(R_*)$)	2 – 3	2.0 (0.02 AU)
Outer radius ($\omega_N(R_*)$)	4 – 30	4.0 (0.04 AU)
Acceleration parameter (β)	1 – 7	5
Mass load parameter (γ)	1 – 5	3
Mass loss rate ($\dot{M}_w(M_\odot/yr)$)	10^{-8} – 10^{-7}	5×10^{-8}

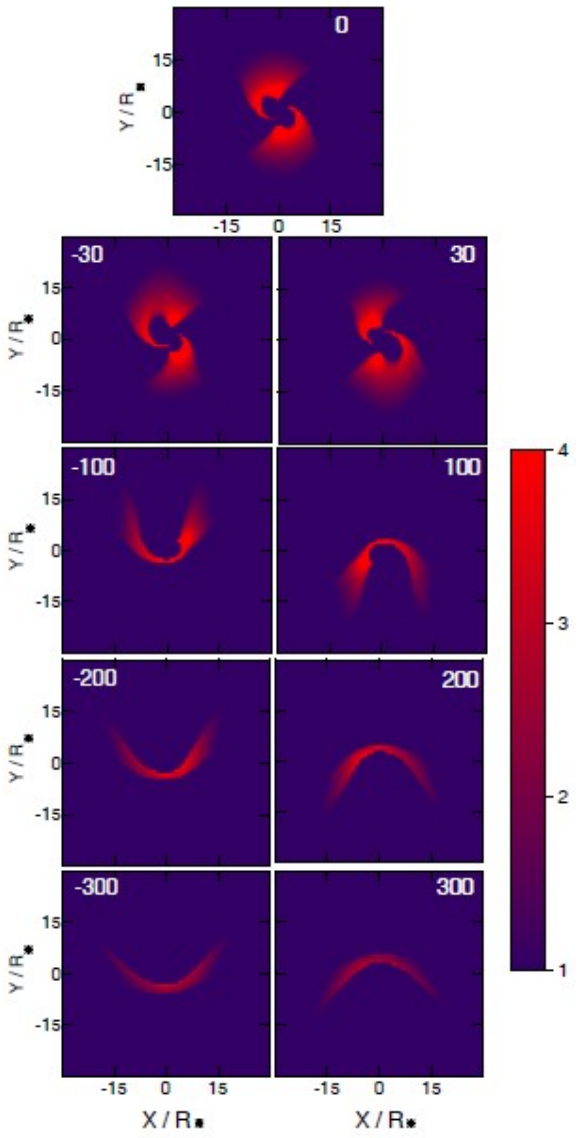

Disk wind images
at different radial velocities

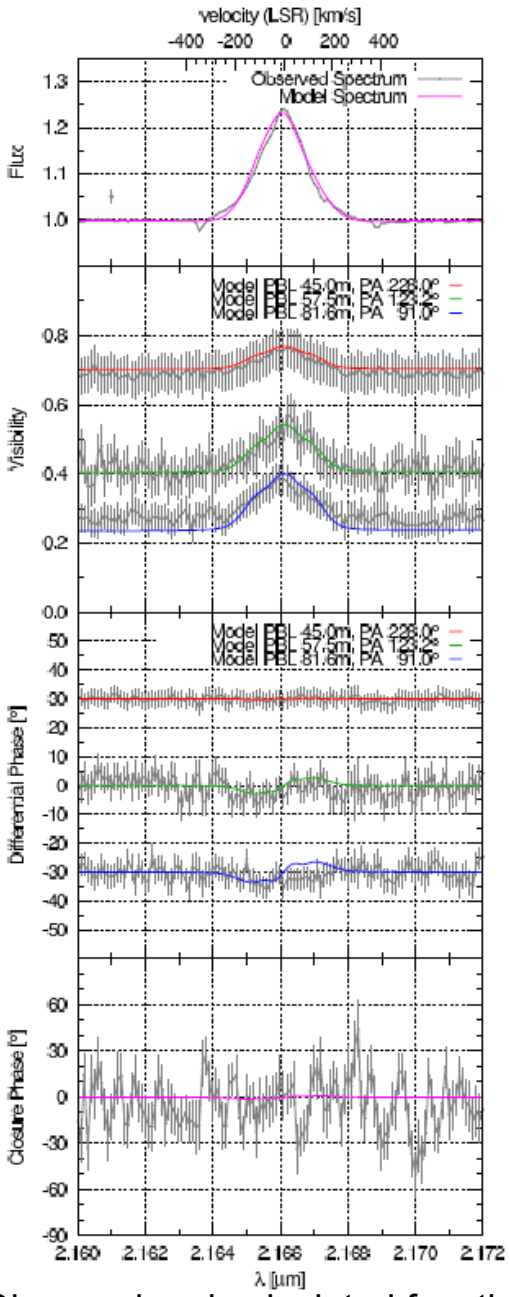

Observed and calculated functions

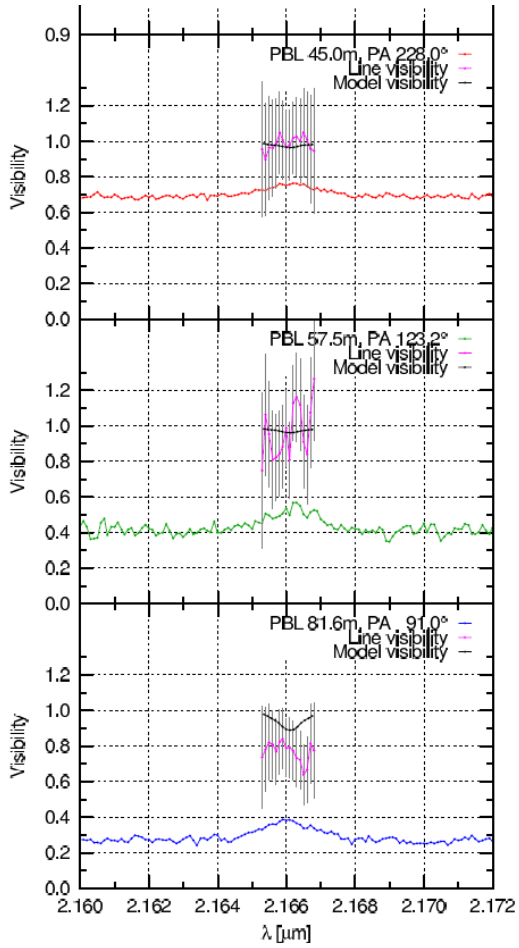

Pure line visibilities

Ferreira et al. 2006

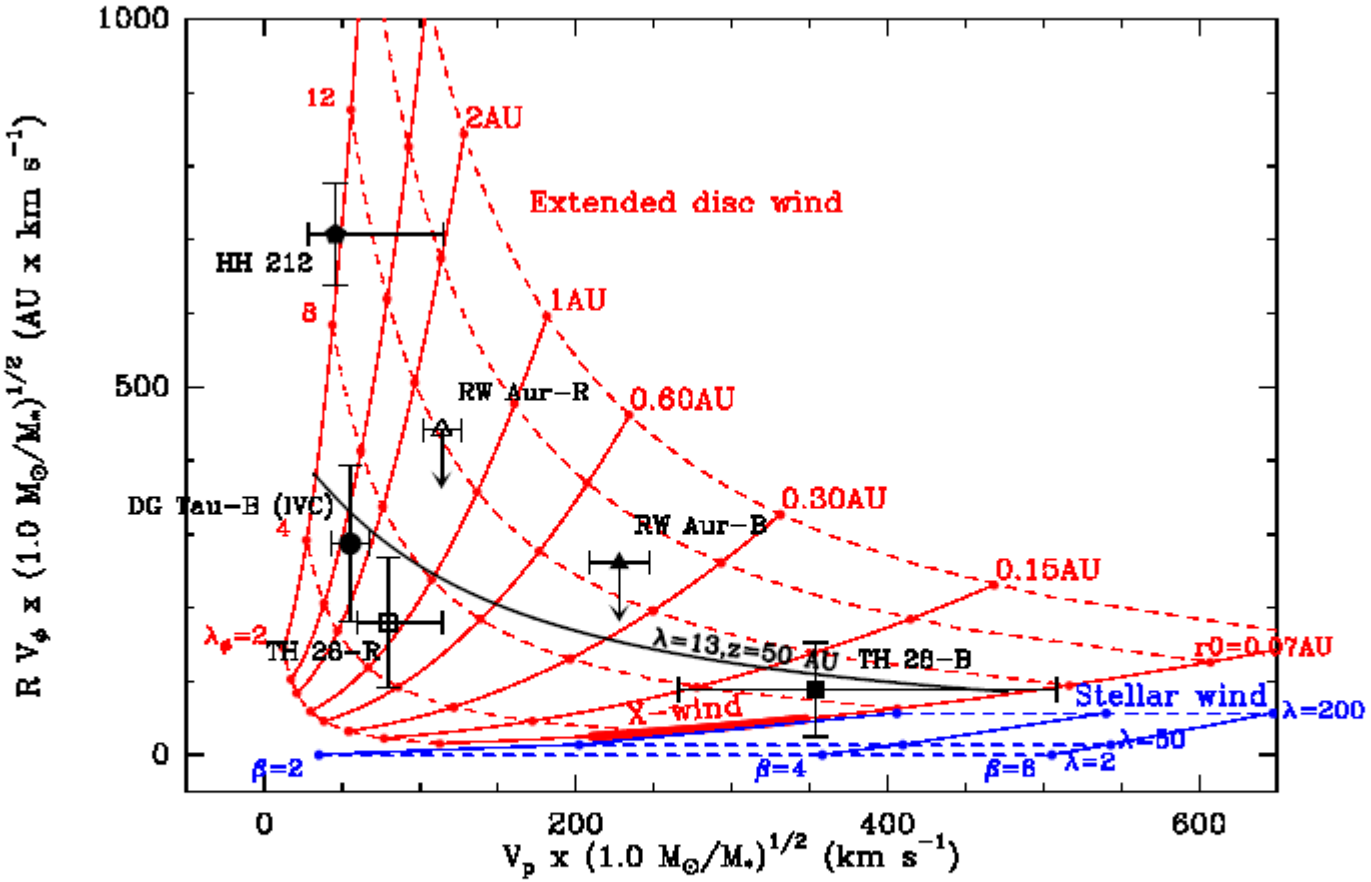

Fig. 3. Comparison of predicted specific angular momentum vs. poloidal velocities with observations of T Tauri microjets. Full and dashed curves show expected theoretical relations for MHD disc and stellar winds (same as Fig. 2, on a linear scale). Plotted in symbols are jet kinematics measured at distance $z \simeq 50$ AU in the DG Tau, RW Aur, and Th 28 jets. The infrared HH 212 jet is also shown for comparison. See text for more details on how the data points and their associated error bars are computed.

MWC 480

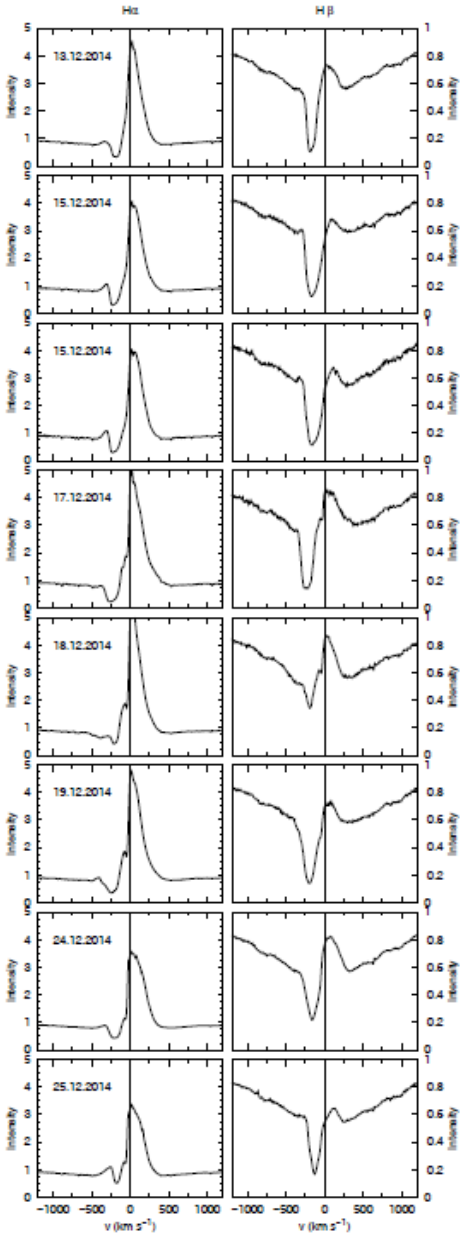

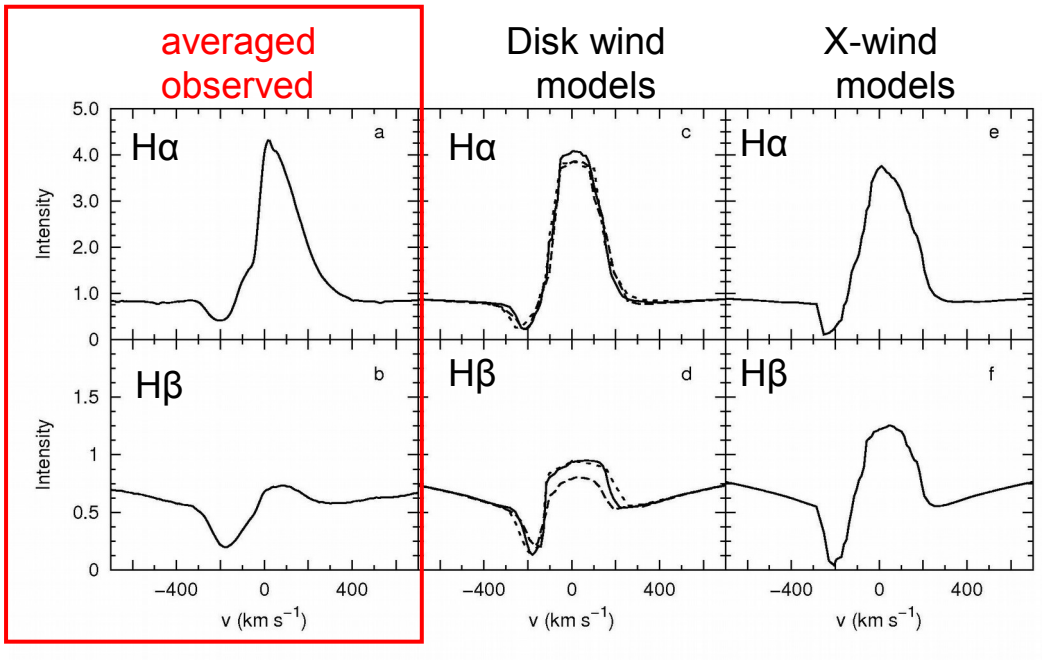

Calculated Hα (c) and Hβ (d) line profiles with the disk wind models (i = 47 - 55°)

Calculated Hα (e) and Hβ (f) line profiles with the X-wind model (i = 52°)

CO, CN emission: i ~ 30° – 38°, but Hα radial vel.: 45±6° (Grady et al. 2010)

Mendigutia + 2013 (X-Shooter):

our work:

$$\dot{M}_{DW}/\dot{M}_{acc} \approx 0.1$$

$$\dot{M}_{accr} = (0.8 - 1.9) \cdot 10^{-7} M_{\odot}/yr$$

$$\dot{M}_{DW} = 2.5 \cdot 10^{-8} M_{\odot} yr^{-1}$$

Grinin et al. 2017, Tambovtseva et al. 2016

Kraus et al. 2008 A&A

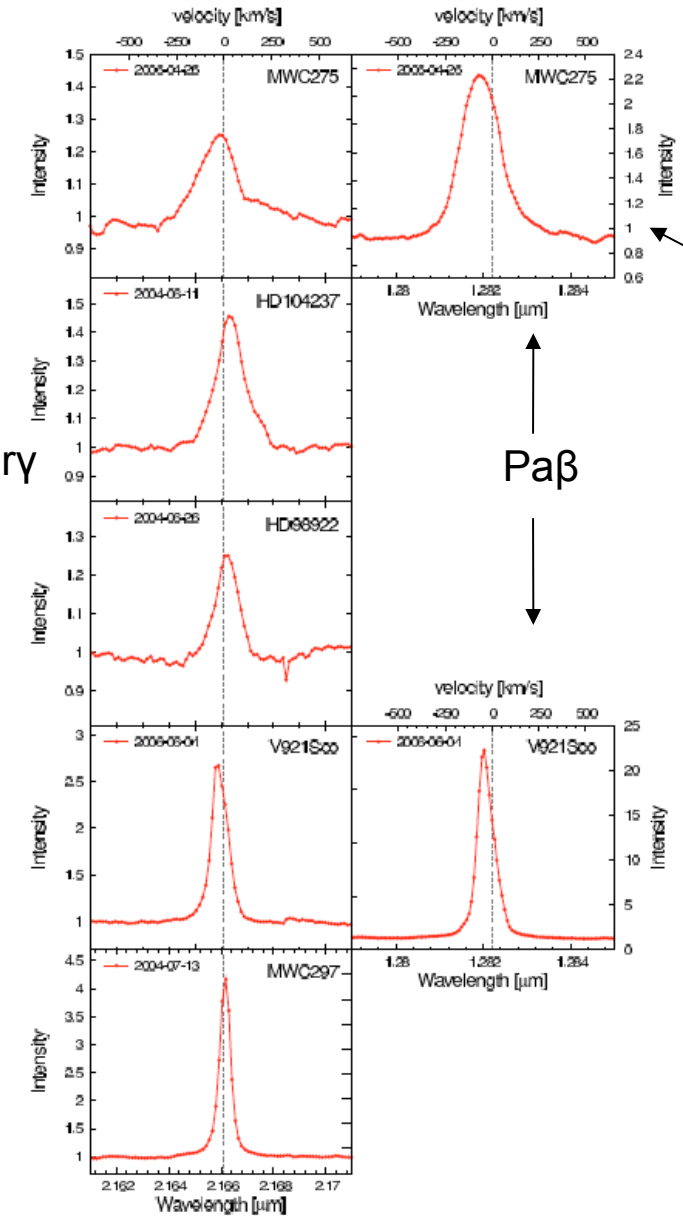

Brγ

Paβ

Hα

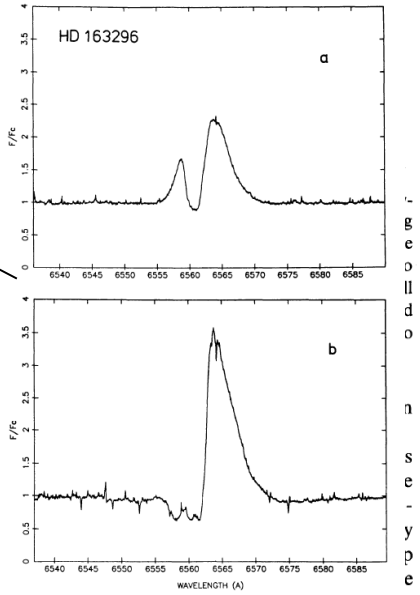

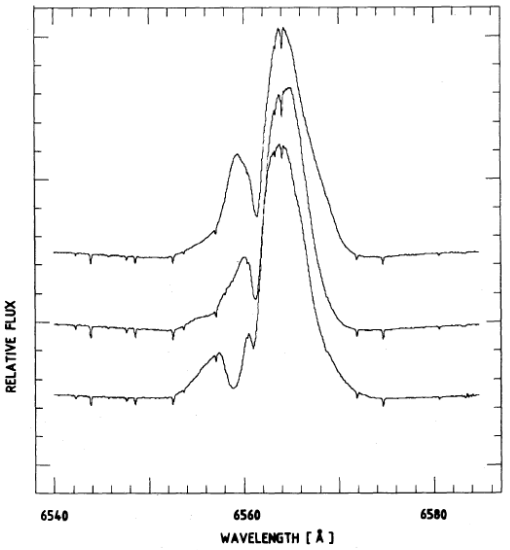

Fig. 3. a) The Hα-emission line of HD 163296 obtained in June 1983. b) The same line observed in September 1983. Note the dramatic change in its intensity as well as in its profile compared to the June spectrum

Fig. 6. Nightly mean Hα profiles of HD 163296 (from top to bottom: 1987 June 7, 8, and 9). The vertical offset between the profiles is 100% of the continuum flux

The et al. 1985, Baade and Stahl 1989, Mendigutia et al. 2013

Fig. 2. *Left*: VLT/ISAAC spectra showing the Brγ line with a spectral resolution of $R \sim 9000$ for the stars in our sample. *Right*: VLT/ISAAC spectra of the Paβ line were obtained for HD 163296 and V921 Sco.

TTSs

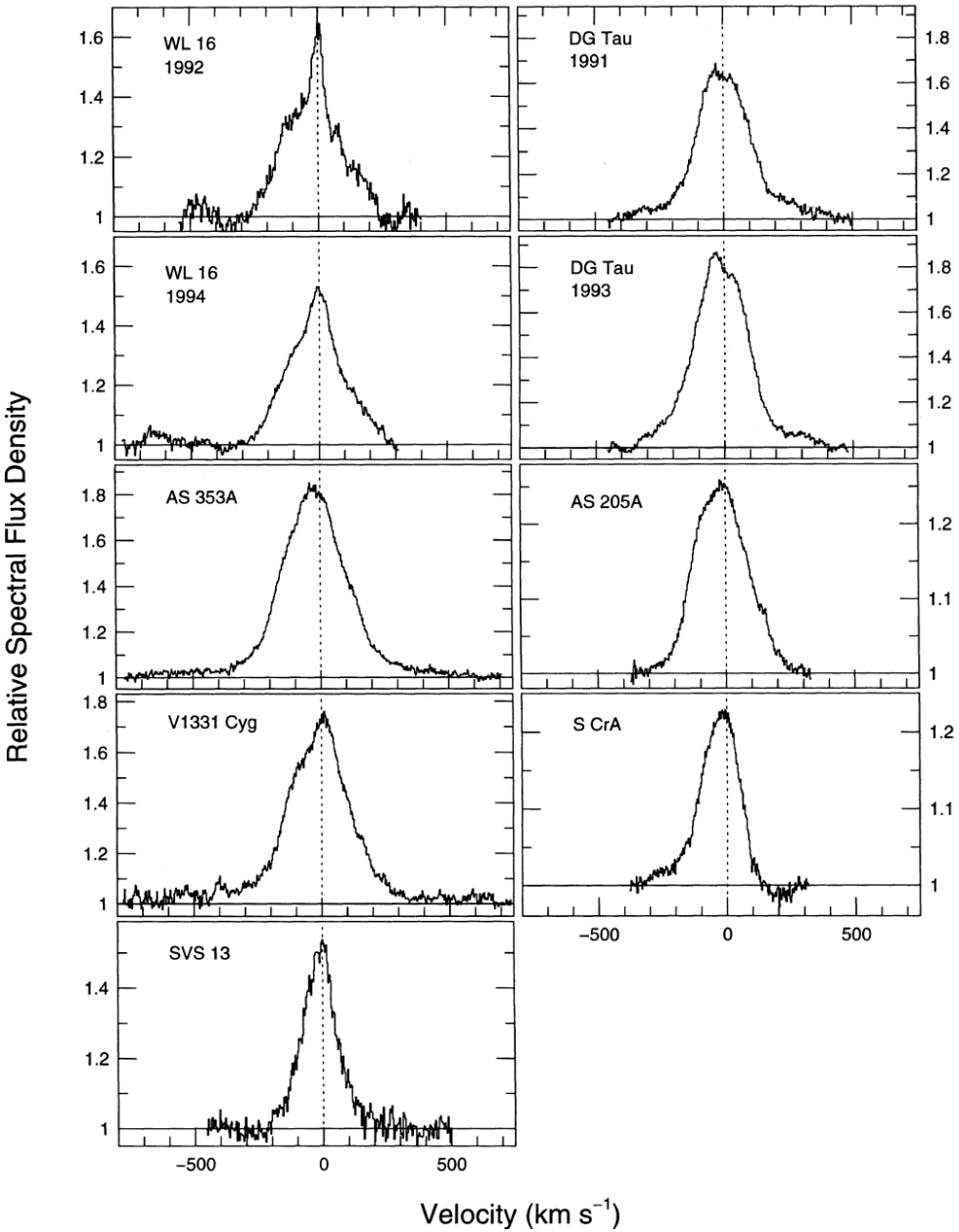

Najita + 1996

The Brγ spectra presented in this paper were obtained during various observing runs from 1991 to 1994 at the NASA Infrared Telescope Facility using CSHELL, the facility near-infrared echelle spectrograph (Tokunaga et al. 1990; Greene et al. 1993).